

Low Depth Quantum Circuits for Ising Models

S. Iblisdir¹, M. Cirio², O. Boada¹ and G.K. Brennen²

¹Dept. Estructura i Constituents de la Matèria, Universitat de Barcelona, 08028 Barcelona, Spain

²Centre for Engineered Quantum Systems, Department of Physics and Astronomy, Macquarie University, North Ryde, NSW 2109, Australia

Abstract

A scheme for measuring complex temperature partition functions of Ising models is introduced. In the context of ordered qubit registers this scheme finds a natural translation in terms of global operations, and single particle measurements on the edge of the array. Two applications of this scheme are presented. First, through appropriate Wick rotations, those amplitudes can be analytically continued to yield estimates for partition functions of Ising models. Bounds on the estimation error, valid with high confidence, are provided and shown to be compatible with previous results. Interestingly, the kind of state preparations and measurements involved in this application can in principle be made “instantaneous”, i.e. independent of the system size or the parameters being simulated. Second, the scheme allows to accurately estimate some non-trivial invariants of links. A third result concerns the computational power of estimations of partition functions for real temperature classical ferromagnetic Ising models on a square lattice. We provide conditions under which estimating such partition functions allow to reconstruct scattering amplitudes of quantum circuits making the problem BQP-hard. Using this mapping, we show that wavefunction overlaps for ground states of quantum Hamiltonians, which can serve as a witness to quantum phase transitions, can be estimated from classical Ising model partition functions. Finally, we show that the ability to accurately measure corner magnetisations on thermal states of two-dimensional Ising models with magnetic field leads to fully polynomial random approximation schemes (FPRAS) for the partition function. Each of these results corresponds to a section of the text that can be essentially read independently.

1 Introduction

Statistical Mechanics provides formal recipes to study interacting many-body systems. Quantities that can be experimentally probed, such as the free energy or the specific heat, can in principle be derived straightly. More often than not, though, computing these quantities turns out to be impossible. As can be seen from very idealised systems, our ability to actually apply these recipes is very limited. During the last ten years, significant efforts have been devoted to investigating whether quantum mechanics could help in this respect. Various methods, all involving the superposition principle, have been proposed to compute the Jones polynomial at particular values of its variable [1], partition functions of classical statistical models [2, 3], the Tutte polynomial [4], or more generally to contract tensor networks [3].

In this work, we will mainly focus on a collection of *classical* two-level systems, each attached to a fixed position corresponding to a vertex of some lattice Λ , with edges $E(\Lambda)$. The state of a particle located at vertex i is associated with a number σ_i taking value in $\{-1, +1\}$. The energy of the system is given by an Ising Hamiltonian function, associating an energy with each classical configuration of the system σ_Λ :

$$H(\sigma_\Lambda) = - \sum_i h_i \sigma_i - \sum_{\langle i,j \rangle} J_{i,j} \sigma_i \sigma_j. \quad (1)$$

The first sum in this equation runs over all vertices of Λ . The quantity h_i models represents some local field felt by a spin located at position i . The second sum represents interactions between pairs of neighbour particles (edges of the lattice). The strength and sign of these interactions may vary from pair to pair. This model was introduced by Lenz as an idealisation of systems where magnetic interactions prevail [5]. Although innocent looking, it exhibits an extremely rich structure. On a regular lattice, close to a phase transition, its long range behaviour is similar to that of very interesting field theories [6] while the problem of computing its partition function,

$$Z(\beta) = \sum_{\{\sigma\}} \exp[-\beta H(\{\sigma\})], \quad (2)$$

belongs the NP-hard complexity class [7].

It is the purpose of this paper to present schemes that allows to accurately estimate $Z(\beta)$ for imaginary values of β (Section 2), through manipulation of a suitable quantum mechanical system. Quantum circuits for this task have been previously proposed in Ref.[8]. However with our scheme, we will see how to evaluate partition functions of real systems, through analytic continuation (Section 4). As we shall see, the kind of preparation and measurement necessary for this estimation can in principle be made *in constant time*, i.e. independent of the system size or the parameters being simulated. This feature is particularly appealing in view of possible practical implementations. We will then see that imaginary temperature partition functions are interesting in their own right, because they provide non-trivial invariant of knots (Section 5). Section 6.1 deals with computational complexity issues. We investigate the (quantum) computational power of the Ising model, and show how the ability to estimate real temperature partition functions of this model allows to efficiently simulate a quantum computer. One application of this is the estimation of the wavefunction overlap between ground states of a quantum Hamiltonian in the vicinity of a quantum phase transition. We also show that some much simpler tasks have computational power. In particular, the ability to detect corner magnetisations of disordered Ising models leads to fully polynomial random approximation schemes thereof. Many of the quantum algorithms presented here involve repetitions of either constant depth or linear depth circuits and moreover many of the operations can be performed without individual qubit addressability. This is potentially a real boon to experimental implementations in architectures such as trapped atoms in optical lattices or superconducting qubit arrays where individual addressing is not so easy but many qubits are available. In addition some of the circuits provide for a trade off in space and time, i.e. one can perform either constant depth circuits in $d + 1$ spatial dimensions or linear depth circuits in d dimensions. Constant depth quantum circuits have attracted attention since the discovery of simple examples (depth-1 circuits) that are expected to be difficult to simulate classically [9]. Furthermore, there is some evidence that fault tolerance thresholds could be improved for constant depth (or more generally logarithmic depth) quantum circuits [10, 11].

2 Complex temperature partition functions

We wish to study a classical system defined on some d -dimensional lattice Λ . For that purpose, we consider an associated situation, where a two-level system is located on each vertex of Λ . The computational basis for each quantum particle, $\{|+\rangle, |-\rangle\}$, will be associated with classical individual spin configurations. Our construction relies on controlled phase gates acting on nearest neighbours, that is, elements $\langle k, l \rangle$ of $E(\Lambda)$, the set of edges of the lattice. Their action is best described in computational basis:

$$C_{k,l} : |\sigma_k, \sigma'_l\rangle \rightarrow e^{i\phi_{k,l}(\sigma_k, \sigma'_l)} |\sigma_k, \sigma'_l\rangle. \quad (3)$$

Importantly, these phase gates all commute with each other:

$$\forall \langle k, l \rangle, \langle x, y \rangle \in E(\Lambda), \quad [C_{k,l}, C_{x,y}] = 0. \quad (4)$$

Obviously, each function $\phi_{\langle k,l \rangle}$ can be expressed as

$$\phi_{\langle k,l \rangle}(\sigma_k, \sigma'_l) = \sum_{s=\pm 1} \sum_{s'=\pm 1} \phi_{k,l}(s, s') \delta_{s\sigma_k} \delta_{s'\sigma'_l}.$$

With the definitions $\kappa_k \equiv \frac{1}{4} \sum_{s_k, s_l} \phi_{k,l}(s_k, s_l)$, $J_{k,l} \equiv \frac{1}{4} \sum_{s_k, s_l} \phi_{k,l}(s_k, s_l) s_k s_l$, $h_k \equiv \frac{1}{4} \sum_{s_k, s_l} \phi_{k,l}(s_k, s_l) (s_k + s_l)$, we see that a collective action of controlled phase gates across all edges of the lattice can be described, in computational basis, as¹

$$\prod_{\langle k,l \rangle \in E} C_{k,l}^\alpha \prod_{k \in \Lambda} |\sigma_k\rangle = \exp \left[i\alpha \sum_{k \in \Lambda} \kappa_k + i\alpha \sum_{k \in \Lambda} h_k \sigma_k + i\alpha \sum_{\langle k,l \rangle \in E} J_{k,l} \sigma_k \sigma_l \right] \prod_{k \in \Lambda} |\sigma_k\rangle. \quad (5)$$

In particular, if each quantum particle is initialised in the state

$$|+_x\rangle \equiv \frac{1}{\sqrt{2}}(|+\rangle + |-\rangle), \quad (6)$$

we see that the mean value of a product of phase gate operators takes the form of a partition function at imaginary temperature $i\alpha$:

$$A(\alpha) \equiv \langle +_x^{\otimes |\Lambda|} | \prod_{\langle k,l \rangle \in E} C_{kl}^\alpha | +_x^{\otimes |\Lambda|} \rangle = \frac{1}{2^{|\Lambda|}} \sum_{\{\sigma\}} e^{-i\alpha H(\sigma)}, \quad (7)$$

with H of the form given by Eq.(1).

It is actually **possible** to get partition functions of a classical $(d+1)$ -dimensional system through evolution of a d -dimensional quantum system. For that, we use two additional kinds of gates besides the controlled phase gate. The first kind is single qubit rotations:

$$\begin{aligned} U_k : |+\rangle &\rightarrow \cos \theta_k |+\rangle + \sin \theta_k |-\rangle, \\ U_k : |-\rangle &\rightarrow -\sin \theta_k |+\rangle + \cos \theta_k |-\rangle. \end{aligned} \quad (8)$$

As discussed in Appendix A, other choices are possible. The second is single qubit phase gate:

$$P_k(\varphi_k) : |\sigma_k\rangle \rightarrow e^{i\varphi_k \sigma_k} |\sigma_k\rangle. \quad (9)$$

Next, we observe that the matrix elements of U_k can be expressed in exponential form for almost all values of the parameters θ_k :

$$\langle \sigma'_k | U_k | \sigma_k \rangle = \exp \left[J_k^\downarrow \sigma_k \sigma'_k + i\frac{\pi}{4} \sigma'_k - i\frac{\pi}{4} \sigma_k + B(\theta_k) \right], \quad \theta_k \notin \{k\frac{\pi}{2} : k \in \mathbb{Z}\}, \quad (10)$$

where

$$J_k^\downarrow = -\frac{1}{2} \ln(\tan \theta_k) - i\frac{\pi}{4}, \quad (11)$$

and

$$B(\theta_k) = \frac{\ln(\cos(\theta_k))}{2} + \frac{\ln(\sin(\theta_k))}{2} + i\frac{\pi}{4}. \quad (12)$$

These individual rotations $\{U_k, k \in \Lambda\}$ are applied on all lattice sites simultaneously. For bookkeeping, it is convenient to assume there is an external clock recording the moment t where simultaneous rotations are

¹Note to a reader interested in reproducing the calculations: the identity $\delta_{\sigma\sigma'} = \frac{1+\sigma\sigma'}{2}$ has been repeatedly used.

applied, and ticking at exactly this time. There is nothing particular to this clock, it is just a way to label the change of variables necessary to describe the action of the U_k gates:

$$\prod_{k \in \Lambda} U_k(t) |\sigma(t)\rangle = G(t) \sum_{\{\sigma(t+1)\}} \exp \left[\sum_{k \in \Lambda} J_k^\dagger(t) \sigma_k(t) \sigma_k(t+1) + i \frac{\pi}{4} \sum_{k \in \Lambda} (\sigma_k(t+1) - \sigma_k(t)) \right] |\sigma(t+1)\rangle, \quad (13)$$

where $G(t) = \exp(\sum_{k \in \Lambda} B(\theta_k(t)))$.

Now let us consider a d -dimensional lattice Λ of particles each prepared in the state (6). Let us assume that a layer evolution operator

$$\mathcal{L}(t) = \prod_{k \in \Lambda} P_k(-\frac{\pi}{4}) \prod_{k \in \Lambda} U_k(t) \prod_{\langle k, l \rangle \in E} C_{k, l}^\alpha(t) \prod_{k \in \Lambda} P_k(\frac{\pi}{4}). \quad (14)$$

is applied $(m-1)$ times on this initial state, leading to the final state $\prod_{t=1}^{m-1} \mathcal{L}(m-t) |+_x\rangle^{\otimes |\Lambda|}$ (see Fig.1).

The overlap of this state with the initial state $|+_x^{\otimes |\Lambda|}\rangle$ takes again the form of an Ising partition function, but now defined on an enlarged lattice $\hat{\Lambda} = \Lambda \times \{1, \dots, m\}$:

$$A(\alpha, \Theta) \equiv \langle +_x^{\otimes |\Lambda|} | \prod_{t=1}^{m-1} \mathcal{L}(m-t) |+_x^{\otimes |\Lambda|} \rangle = \frac{1}{2^n} \sum_{\sigma} \exp[-H(\sigma)], \quad (15)$$

where, Θ denotes collectively all individual rotations performed on the system, and where, up to an additive constant $\sum_{t=1}^m \ln G(t)$, the classical hamiltonian H is given by

$$-H(\sigma) = i\alpha \sum_{t=1}^m \sum_{k \in \Lambda} h_k(t) \sigma_k(t) + i\alpha \sum_{t=1}^m \sum_{\langle k, l \rangle \in E} J_{k, l}(t) \sigma_k(t) \sigma_l(t) + \sum_{t=1}^{m-1} \sum_{k \in \Lambda} J_k^\dagger(t) \sigma_k(t) \sigma_k(t+1). \quad (16)$$

Eq.(15) is proven by inserting identity operators and identifying single-particle quantum basis states $|\pm\rangle$ with single particle classical spin configurations $|\sigma\rangle$:

$$\langle +_x^{\otimes |\Lambda|} | \prod_{t=1}^{m-1} \mathcal{L}(m-t) |+_x^{\otimes |\Lambda|} \rangle = \frac{1}{2^n} \sum_{\sigma(1) \dots \sigma(m)} \prod_{t=1}^{m-1} \langle \sigma(m-t+1) | \mathcal{L}(m-t) | \sigma(m-t) \rangle.$$

3 Implementation

At the core of the discussion held in the previous section lies the ability to measure the scalar product between n -particle states $|\Phi\rangle$ and $|\Psi\rangle$. We will describe two measurement protocol addressing this problem. The first is the simpler and allows to detect $|\langle \Phi | \Psi \rangle|^2$, while the second truly yields $\langle \Phi | \Psi \rangle$.

Protocol 1

1. Prepare an n -particle system A in the state $|\Psi\rangle$, and an n -particle system B in the state $|\Phi\rangle$.
2. Prepare an ancillary register R of n qubits in the state $|GHZ\rangle = \frac{1}{\sqrt{2}}(|+\dots+\rangle + |-\dots-\rangle)$.
3. Perform a bit-wise controlled swap gate with each qubit R_j of the register as a control and A_j, B_j as targets, i.e. if qubit R_j is in the state $|-\rangle$ then apply $\text{SWAP}(A_j, B_j)$. We get

$$\frac{1}{\sqrt{2}} \left(|+\dots+\rangle_R |\Psi\rangle_A |\Phi\rangle_B + |-\dots-\rangle_R |\Phi\rangle_A |\Psi\rangle_B \right)$$

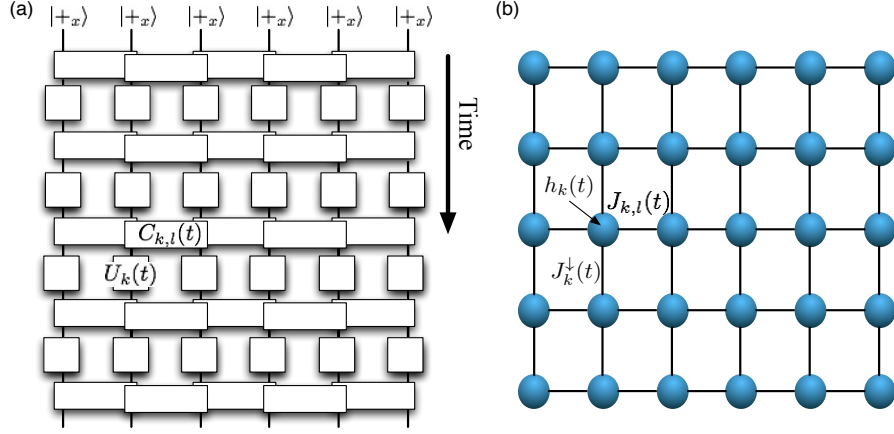


Figure 1: Example of the quantum algorithm on a 1D chain of qubits to compute the partition function of a 2D classical Ising model at imaginary temperature. (a) The quantum algorithm begins with qubits in the chain initialized in state $|+x\rangle$ and proceeds with alternating sequences of parallel nearest neighbour two qubit gates $C_k(t)$ diagonal in the computational basis $\{|\pm\rangle\}$ and parallel local rotations $U_k(t)$ (supplemented by single qubit phase gates). (b) The corresponding classical Ising model with spatially dependent horizontal and vertical bond strengths and local magnetic fields.

4. Measure the first $n - 1$ qubits of R in the basis $\{|\pm_x\rangle\} = \{\frac{1}{\sqrt{2}}(|+\rangle \pm |-\rangle)\}$. Denote $m_j = \pm 1$ the (equiprobable) outcomes of measurement on register qubit j and define $\chi = \sum_{j=1}^{n-1} m_j$. The state for the last qubit of the register and the system AB is

$$\frac{1}{\sqrt{2}} \left(|+, \Psi, \Phi\rangle + (-1)^\chi |-, \Phi, \Psi\rangle \right). \quad (17)$$

5. Measure the Pauli operator σ^x of the last ancillary qubit R_n . The expectation value is

$$\langle \sigma_n^x \rangle = (-1)^\chi |\langle \Phi | \Psi \rangle|^2. \quad (18)$$

Protocol 2

1. Prepare an n -particle system A in the state $|\Phi\rangle$.
2. Prepare an ancillary register R of n qubits in the GHZ state
3. Evolve the qubits in register A conditioned on the state of the ancilla to prepare

$$\frac{1}{\sqrt{2}} \left(|+\dots+\rangle_R |\Phi\rangle_A + |-\dots-\rangle_R |\Psi\rangle_A \right)$$

This can be done by replacing all instances of quantum gates in the evolution of $|\Phi\rangle \rightarrow |+\otimes_x^n\rangle \rightarrow |\Psi\rangle$ into bitwise controlled gate operations. The single qubit phase gates become controlled phase gates: $|+\rangle_{R_k} \langle +| \otimes \mathbf{1}_{A_k} + |-\rangle_{R_k} \langle -| \otimes P_{A_k}$. Similarly, the single qubit rotations become: $|+\rangle_{R_k} \langle +| \otimes \mathbf{1}_{A_k} + |-\rangle_{R_k} \langle -| \otimes U_{A_k}$. The collisional gates are controlled by one of neighboring ancillary qubits, e.g.: $|+\rangle_{R_x} \langle +| \otimes \mathbf{1}_{A_x, A_y} + |-\rangle_{R_k} \langle -| \otimes C_{A_x, A_y}$. Such three qubit diagonal gates can be decomposed into at most 6 nearest neighbor controlled phase gates [12].

4. Measure the first $n-1$ qubits of R in the basis $\{|\pm_x\rangle\}$. Denote $m_j = \pm 1$ the outcome of measurement on register qubit j and let again $\chi = \sum_{j=1}^{n-1} m_j$. The state for the last qubit of the register and the system A is

$$\frac{1}{\sqrt{2}} \left(|+, \Phi\rangle + (-1)^\chi |-, \Psi\rangle \right). \quad (19)$$

5. Measure σ^x on the last ancillary qubit R_n . The expectation value is

$$\langle \sigma_n^x \rangle = (-1)^\chi \Re[\langle \Phi | \Psi \rangle]. \quad (20)$$

6. Repeat steps 1-4 but on the last qubit R_n measure instead the Pauli operator σ^y where the basis $\{|\pm_y\rangle\} = \{\frac{1}{\sqrt{2}}(|+\rangle \pm i|-\rangle)\}$. The expectation value is

$$\langle \sigma_n^y \rangle = (-1)^\chi \Im[\langle \Phi | \Psi \rangle]. \quad (21)$$

We note that it is actually not necessary to prepare size n ancillary registers in a GHZ state for either measurement protocol, since one ancillary qubit making controlled swaps or controlled interactions like a serial tape head over the quantum registers would suffice. The penalty is a potentially linear slowdown and the need to transport the ancilla qubit over the register for every gate in the circuit. The $|GHZ\rangle$ state can be prepared in one plane using global, i.e. spatially homogeneous, pulses in the plane [13, 14, 15]. Furthermore, by coupling the quantum register with a common bosonic mode, $|GHZ\rangle$ states can be prepared in constant time [16]. The idea is to place all the spins inside a high Q cavity (with decay rate κ) with a resonance field frequency close to the transition between the qubit states and some other excited state. When the coupling between the field and qubits is spin dependent and dispersive (e.g. a differential light shift induced by polarization selection rules or by spin dependent detuning) then the interaction is modelled as:

$$V_z = g_z a^\dagger a \sum_j \sigma_j^z, \quad (22)$$

where g_z is the dispersive coupling strength. Then $|GHZ\rangle$ can be produced either using strong coupling with a quantised state of light or via a geometric phase gate using coherent state displacements. We outline the latter as follows:

- Initialize all the spins in $|+_x\rangle$ and the cavity mode in the vacuum state $|\alpha = 0\rangle$.
- Perform the following nine step interaction sequence:

$$D(-\beta^{-\kappa\tau}) e^{-i\tau V_z} D(-\alpha^{-\kappa\tau}) \left[\prod_j \sigma_j^x \right] e^{-i\tau V_z} \left[\prod_j \sigma_j^x \right] D(\beta) e^{-i\tau V_z} D(\alpha),$$

where $D(\alpha) = e^{\alpha a^\dagger - \alpha^* a}$ is a coherent state displacement, and $e^{-i\tau V_z}$ is the unitary evolution generated by V_z . When the parameters satisfy: $g_z \tau = \pi/2$, and $|\alpha\beta|(e^{-3\kappa\tau/2} + e^{-\kappa\tau/2}) = \pi/4$, then the cavity returns to the vacuum and the global rotation $U = e^{-i\frac{\pi}{4} \prod_j \sigma_j^z}$ is applied to the qubits.

- Apply the global operation $\prod_j e^{i\frac{\pi}{2\sqrt{2}}(\sigma_j^x + \sigma_j^z)}$ to the spins.

The state of the qubits is then $\frac{1}{\sqrt{2}}(|++\dots+\rangle - i|--\dots-\rangle)$ which is locally equivalent to $|GHZ\rangle$ and functions just as well for the simulation protocols above. The overall process fidelity, which measures how close the lossy process is to the target unitary $U = e^{-i\frac{\pi}{4} \prod_j \sigma_j^z}$, satisfies [17]

$$F_{\text{pro}} \geq 1 - \frac{\pi^2 \kappa}{2|g_z|} \left(1 + \frac{\pi \kappa}{2|g_z|} \right).$$

Note that this is a constant depth circuit thanks to the non-local coupling of the field to the qubits. Of course as the number of spins increases the size of the cavity must also increase, and the strength of the field, spin coupling decreases as $1/\sqrt{Vol}$ where Vol is the cavity volume. Consequently, there is ultimately a process time which scales as \sqrt{n} where n is number of qubits. However, in practice this could be quite fast compared to a sequential circuit for generating $|GHZ\rangle$.

Since the measurement of $\langle\Phi|\Psi\rangle$ is informationally more complete than that of $|\langle\Phi|\Psi\rangle|^2$, the reader might wonder why we have bothered describe a separate procedure to measure the latter quantity. The reason is that the second measurement seems to be experimentally more demanding than the first. The information provided by the first kind of measurement is however certainly valuable and for most of the discussion to follow we assume data is obtained from this kind of measurement.

So far, we have considered the case of planar boundary conditions. If the classical system is periodic in space (i.e. the lattice Λ is periodic) then the above quantum algorithm is simply modified in the couplings $J_{k,l}(t)$ to account for this. If the classical system is periodic in the time direction, then a few modifications are needed. To relate the measurement of the quantum system to the classical partition function, the boundaries states $|\sigma_k(m)\rangle$ and $|\sigma_k(1)\rangle$ must be identified. So rather than computing the scattering matrix element $\langle +_x^{\otimes|\Lambda|} | W | +_x^{\otimes|\Lambda|} \rangle$, where the unitary W is defined as $W = \prod_{t=1}^{m-1} \mathcal{L}(m-t)$, as we have described so far, we want the trace: $\text{Tr}[W]$. This is found by using the measurement protocol 1 but with the register A prepared in the completely mixed state $\frac{1}{2^n}$. The polarization measurements of the last ancilla of the register then yield the real and imaginary parts of $\frac{\text{Tr}[W]}{2^n}$. Also note by the cyclic property of the trace, the phase gates P_k are no longer needed in the quantum evolution.

Consider the implementation of this measurement for a 3D classical Ising model using a quantum register encoded in a plane. For protocol 1 three parallel planes are needed, one (the top plane) prepared in a $|GHZ\rangle$ state, and the centre (c) and bottom (b) planes both prepared in $|+_x^{\otimes n}\rangle$. The centre plane is prepared in $\prod_{\langle k,l \rangle \in E} C_{k,l}^\alpha |+_x^{\otimes|\Lambda|}\rangle$ or evolved in $\prod_{t=1}^{m-1} \mathcal{L}(m-t) |+_x^{\otimes|\Lambda|}\rangle$, and the subsequent C-SWAP gates between registers can be implemented in parallel bitwise between pairs (c_k, b_k) using a sequence of at most 12 nearest neighbor collisional gates [12]. Finally the measurement of the top register only requires collecting the parity of measurement outcomes of $n-1$ qubits in the bulk (without addressability) and an addressable measurement of X_n for one qubit on a corner. For protocol 2 two registers are needed: the top one prepared in $|GHZ\rangle$ state and the bottom prepared in $|+_x^{\otimes n}\rangle$. During the quantum evolution all gates acting on the bottom register (say qubit b_k) are to be controlled by the neighbouring qubit on the top plane (qubit t_k). For a rotation gates $U_k(t)$ this means to instead apply the controlled gate $|+\rangle_{t_k} \langle +| \otimes \mathbf{1}_{b_k} + |-\rangle_{t_k} \langle -| \otimes U_k(t)$. Such a gate can be done using at most 3 controlled collision gates between t_k and b_k . For the two qubit gates $C_{k,l}(t)$ we need to apply $|+\rangle_{t_k} \langle +| \otimes \mathbf{1}_{b_k, b_l} + |-\rangle_{t_k} \langle -| \otimes C_{k,l}(t)$. This three qubit diagonal gate can be realized using at most 12 collisional gates between nearest neighbors t_k, b_k and b_k, b_l . Since not all the gates now commute it is necessary to do this in two stages over non overlapping pairs of nearest neighbors in the bottom register. Measurement of the top register proceeds as for protocol 1. Regarding addressability, it is necessary to be able to address the different planes along \hat{z} but addressability can be relaxed in the $\hat{x} - \hat{y}$ direction.

4 Partition functions

The schemes of Section 2 can be used to provide estimates for real temperature partition functions of classical models. We proceed by analytic continuation of the quantum amplitudes (or their modules) provided by the protocols described in Section 2. The general idea is to view the partition function as a polynomial of order linear in the system size whose coefficients are the same as the those obtained from the quantum amplitude estimation but with real instead of complex variables, and then to Wick rotate these variables.

Let α and θ denote two *complex* variables, and consider a function F of the form

$$F : \mathbb{C} \times \mathbb{C} \rightarrow \mathbb{C} : (\alpha, \theta) \rightarrow F(\alpha, \theta) = \sum_{\nu_1=-N_1}^{N_1} \sum_{\nu_2=-N_2}^{N_2} c_{\nu_1, \nu_2} e^{i\nu_1 \alpha} e^{i\nu_2 \theta}, \quad (23)$$

where $N_1, N_2 < \infty$. Clearly, F is an *analytic* function, so the coefficients $\{c_{\nu_1, \nu_2}\}$ define F on the whole complex plane. If F is known for $\alpha_{j_1} = \alpha^{(j_1)} = 2\pi \frac{j_1}{N_1}$, $j_1 = 0 \dots 2N_1$, $\theta_{j_2} = \theta^{(j_2)} = 2\pi \frac{j_2}{N_2}$, $j_2 = 0 \dots 2N_2$, then a Fourier transform yields

$$c_{\nu_1 \nu_2} = \frac{1}{(2N_1 + 1)(2N_2 + 1)} \sum_{j_1=0}^{2N_1} \sum_{j_2=0}^{2N_2} e^{-2i\pi j_1 \nu_1 / (2N_1 + 1)} e^{-2i\pi j_2 \nu_2 / (2N_2 + 1)} F(\alpha_{j_1}, \theta_{j_2}). \quad (24)$$

Plugging this expression in Eq.(23), one finds sums of geometric series. Summing them yields

$$\hat{F}(\alpha, \theta) = \sum_{j_1=0}^{2N_1} \sum_{j_2=0}^{2N_2} F(\alpha_{j_1}, \theta_{j_2}) w^{(N_1)}(\alpha - \alpha_{j_1}) w^{(N_2)}(\theta - \theta_{j_2}), \quad (25)$$

where

$$w^{(N)}(x) \equiv \frac{1}{2N + 1} \frac{\sin((2N + 1)\frac{x}{2})}{\sin \frac{x}{2}}. \quad (26)$$

Now consider the quantum amplitudes introduced in Section 2, in the case where $h_k(t), J_{k,l}(t) \in \{-1, +1\}$, $\forall k \in \Lambda$, $\forall \langle k, l \rangle \in E(\Lambda)$, $\forall t = 1 \dots m$, and where all 'vertical' couplings J^\downarrow are set to -1 . (For the case of non-uniform vertical couplings, see Appendix A.) In that case, these quantum amplitudes are certainly of the form (23), with N_1, N_2 growing at most polynomially with the number of vertices of the classical model being under consideration. For suitable *complex* values of α, θ , the probability amplitude $A(\alpha, \theta)$ of the d -dimensional quantum system can be put in correspondence with the *real* partition function of the $(d + 1)$ -dimensional classical system. Namely, for

$$\alpha^* = i\beta, \quad \theta^* = \frac{1}{i} \ln \sqrt{\frac{1 + e^{2\beta J^\downarrow}}{1 - e^{2\beta J^\downarrow}}}, \quad g(\theta^*) \equiv \frac{1}{2} \ln \sin 2\theta^* + \frac{i\pi}{4} - \frac{1}{2} \ln 2, \quad (27)$$

one finds that $A(\alpha^*, \theta^*) = e^{|\Lambda| m g(\theta^*)} Z^{\text{Ising}}(\beta) / 2^{|\Lambda|}$. In the definition of α^* , we recognise the familiar Wick rotation. The role of the other parameter, θ^* , is to analytically continue the *unitary* quantum mechanical transfer matrix, between successive times, to the (non-unitary) statistical mechanical transfer matrix. In summary, in order to get information about the partition function of a d -dimensional classical system, we estimate the probability amplitude $A(\alpha, \theta)$ for well-chosen values of α and θ . From the collected data, we reconstruct the dependence of the function A on its variables (α, θ) , as just explained. Finally, analytic continuation of the variables (α, θ) to the suitable values (27) yields an estimate for the desired partition function.

Let us analyse the errors appearing when the values $A(\alpha_{j_1}, \theta_{j_2})$ are not known exactly but estimated by some quantities $\varphi_{j_1 j_2}$. The identity (25) allows to get *a priori* error estimate. To simplify the discussion, let us start with the case where partition functions are estimated using a one-time-step protocol. Then, $m = 0$, $N_1 = \text{poly}(|\Lambda|) \equiv N$ and $N_2 = 0$. Defining $\delta\varphi^* = \max\{|\varphi_j - A(\alpha_j)|, j = 0 \dots 2N\}$, we see, through error propagation, that the error at inverse temperature β , $\Delta A(i\beta)$ satisfies

$$\Delta A(i\beta) \leq \sum_{j=0}^{2N} |w^{(N)}(i\beta - \alpha_j)| \delta\varphi^*. \quad (28)$$

In the limit of large values of β , the r.h.s of this equation essentially behaves as $\delta\varphi^* e^{\beta N}$, indicating that the measurement accuracy should grow exponentially small, with the inverse temperature and the size of the system, in order to maintain the error over our estimate for partition function below some fixed prescribed threshold.

A bound on the error independent of β can also be derived easily. Indeed, for the Hamiltonians we are considering, the partition function can be written as

$$Z^{\text{Ising}}(\beta) = \sum_{k=-N}^N \xi_k e^{-k\beta},$$

where all coefficients ξ_k are non-negative integers whose magnitude is at most $2^{m|\Lambda|}$ (number of classical configurations associated with the system). It would therefore be sufficient to be able to estimate these coefficients with a relative accuracy of $2^{-m|\Lambda|}$ in order to be able to reconstruct $Z^{\text{Ising}}(\beta)$ perfectly. The bound appearing on the r.h.s of (28) is independent of the actual values for the link couplings and magnetic fields of the precise Ising model being simulated. We therefore expect it to be pretty loose.

To get a sharper understanding of how errors behave, we made some numerical simulations. In Fig.2 we show how the error behaves by studying different quantities such as the logarithm of the partition function, the energy and the specific heat. In particular we simulated a model with uniform couplings and zero magnetic fields and a model with ± 1 couplings (with 50% probability) and uniform magnetic field. One can appreciate how, in the uniform case, the error over the partition function goes to zero for zero and infinite temperature. In Appendix A, we show that error over each Fourier coefficient ξ_k is well behaved for large and small values of k (close to $\pm N$), but blows up for intermediate values k (close to 0). This fact is consistent with our numerical observations and the well known duality present in this model [18]. For the non-homogeneous case, we have found that the errors in the partition function starts by growing exponentially with β , then remains constant. This observation is consistent with the fact that there is no known low temperature/high temperature duality relation. The errors we have found are also much larger. Our numerics indicate that, in the non-homogeneous case, the magnitude of the partition function is dominated by those ξ_k corresponding to intermediate values of k , much more so than for the homogeneous case.

Previous attempts at using quantum mechanics to compute approximations of partition functions exhibit errors comparable to ours. A quantum algorithm based on Fourier sampling was introduced in [19] to estimate partition functions and free energies of quantum Hamiltonians, which includes the classical Ising model in the case of all diagonal interactions. There it was found that the number Fourier components needed to be sampled scales polynomially with the lattice size, but in order to obtain a multiplicative approximation of the partition function, the requisite accuracy of estimation of each coefficient scaled exponentially with the system size. An algorithm, based on using a quantum computer to contract tensor networks yields similar approximation scales [3]. Even preparing a quantum state which coherently encodes a classical thermal state of an Ising appears to be difficult, e.g. in Ref. [20] the authors provide an algorithm which does so but is exponential in the square root of the system size (see also [21]).

To conclude this section, we study the possibility to use the data provided by the quantum experiments in order to construct a bound for the error on the estimated partition function. Our motivation is that, possibly, the a posteriori error analysis might be finer than the error bounds provided by plain error propagation. To simplify the discussion, we will again restrict ourselves to one-step protocols. Extension to the general case is straightforward. Let us expand the quantity $A(i\beta)$ as

$$A(i\beta) = \sum_{j=0}^{2N} (\Re w^{(N)}(i\beta - \alpha_j) + i \Im w^{(N)}(i\beta - \alpha_j)) (\Re A(\alpha_j) + i \Im A(\alpha_j)), \quad (29)$$

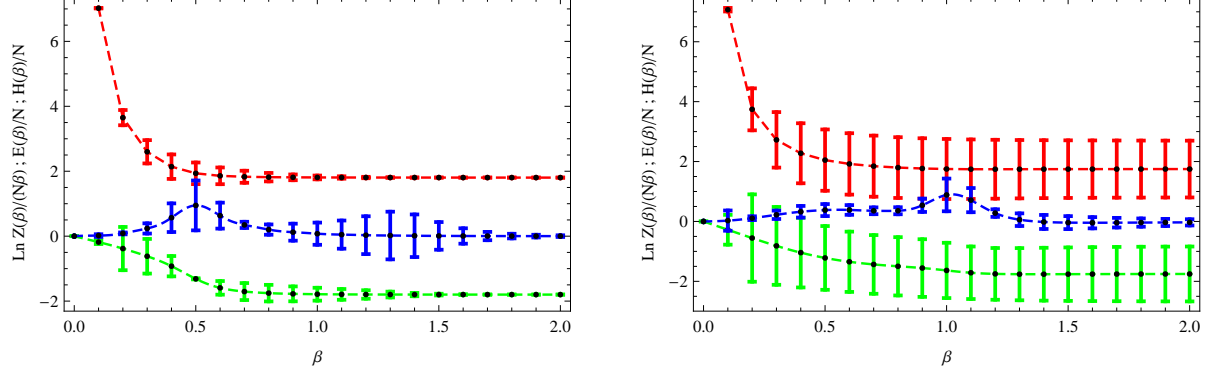


Figure 2: Example of reconstructed quantities for a 10×10 classical Ising model with uniform ferromagnetic couplings ($J = 1$) and zero magnetic field (left) and for a 8×8 classical Ising model with non uniform couplings ($J = \pm 1$ with equal probability) and uniform magnetic field $h = 1$ (right). The reconstructed quantities are the negative of free energy per spin (red), energy (green) and specific heat (blue) as a function of temperature and normalized by the number of spins. The plots show the average value of the quantities mentioned above, which is identical to the true value up to numerical machine precision, with error bars representing the a-priori standard deviation. For the simulation, we supposed to have experimental data with standard deviation equal to 10^{-3} .

and focus on, say,

$$A_{RR}(i\beta) \equiv \sum_{j=0}^{2N} \Re w^{(N)}(i\beta - \alpha_j) \Re A(\alpha_j). \quad (30)$$

The three other bits of $A(i\beta)$ are treated likewise. As was shown in the previous section, each quantity $\Re A(\alpha_j)$ is obtained by measuring the polarisation of a qubit in a precise direction. Such a measurement process can be viewed as drawing a random variable whose outcomes are $\{+1, -1\}$, and whose mean value is the polarisation we are interested in. Let M denote the number of Bernoulli trials involved in determining each probability amplitude, and let us denote $X_j(k)$ the outcome of the k -th trial used in the determination of $\Re A(\alpha_j)$. Our estimate for $A_{RR}(i\beta)$ is

$$\hat{A}_{RR}(i\beta) = \frac{1}{M} \sum_{k=1}^M \sum_{j=0}^{2N} \Re w^{(N)}(i\beta - \alpha_j) X_j(k). \quad (31)$$

For fixed j , the random variables $X_j(k)$ have the same distribution for all k , characterised by $\text{Prob}[X_j(k) = +1] = p_j$. If we assume there is no (uncontrolled) systematic error in the quantum experiments, then the true value of $A_{RR}(i\beta)$ is of course given by

$$A_{RR}(i\beta) = \sum_{j=0}^{2N} \Re w^{(N)}(i\beta - \alpha_j) (2p_j - 1). \quad (32)$$

Let us denote the second moment and third moment of a Bernoulli random variable X respectively as $E_2(X) = \langle (X - \langle X \rangle)^2 \rangle$, $E_3(X) = \langle |X - \langle X \rangle|^3 \rangle$. The following central limit theorem holds for the statistics of errors:

Theorem 4.1 (Central limit) Let $\hat{E}_2(X_j)$ and $\hat{E}_3(X_j)$ denote (appropriate) estimates for $E_2(X_j)$ and $E_3(X_j)$ respectively, obtained from M Bernoulli trials. Then,

$$\forall \delta > 0, \text{Prob} [|\hat{A}_{RR}(i\beta) - A_{RR}(i\beta)| < \delta] \geq$$

$$\sup_{\epsilon > 0} \left(1 - 2 e^{-\frac{M\epsilon}{32}}\right)^{(2N+1)} [1 - 2\mathcal{F}_*(-\lambda_M(\epsilon)\delta) - 1.12 D_M(\epsilon)], \quad (33)$$

where

$$\lambda_M(\epsilon) \equiv \frac{M^{1/2}}{\sqrt{\sum_j (\Re w^{(N)}(i\beta - \alpha_j))^2 (\hat{E}_2(X_j) + \epsilon)^2}}, \quad (34)$$

$$D_M(\epsilon) \equiv \frac{1}{M} \frac{\sum_j |\Re w^{(N)}(i\beta - \alpha_j)|^3 (\hat{E}_3(X_j) + \epsilon)}{[\sum_j (\Re w^{(N)}(i\beta - \alpha_j))^2 (\hat{E}_2(X_j) - \epsilon)]^{3/2}},$$

and where \mathcal{F}_* denotes the cumulative distribution of a zero-mean, unit-variance Gaussian probability distribution.

Proof: The proof of this result builds on the Berry-Essén theorem [22] and is given in Appendix B. \square

5 Link Invariants

There exists several well-established connections between knot theory and statistical mechanics [23]. One of them is the following. For every knot it is possible to construct a graph such that the partition function of a Potts model defined on that graph is a link invariant for certain (imaginary) temperatures. This invariant turns out to be the Jones polynomial evaluated at specific values, modulo a known calculable factor. As the quantum algorithm for computing partition functions described in Section 2 is efficient for imaginary temperatures, it follows that it may also be used to distinguish among different link, when the associated statistical model only involves nearest neighbour interactions. In this section we outline the method to compute the statistical-mechanics knot invariant for any given link. We also compute these invariants for some primary linka with few crossings for which the Potts model involves only a few sites and is within reach of current technology.

Let us start with a brief reminder on a recipe to construct statistical mechanical invariants, given a single component knot or a multicomponent link. We consider the planar projection of a given knot and shade the regions of the diagram in an alternating way such that there are no adjacent shaded regions (there are two ways to do this for any knot). We associate a lattice with vertices \mathcal{V} and signed edges \mathcal{E} , $\Lambda = (E, V)$ to the diagram in the following way. Every shaded region of the diagram will be a vertex of Λ and every crossing of the diagram that separates two shaded regions will be an edge linking the two vertices associated with those regions. The sign for the coupling of the edge is determined by the convention in Fig 3. For every edge $i \in \mathcal{E}$ we associate a weight $\mathcal{W}_i^\pm(\sigma, \sigma')$, where σ, σ' are q -valued spins located at the vertices joined by the edge. Let us define a partition function given a set of weights \mathcal{W}_i on L ,

$$Z_L = \sum_{\{\sigma\}} \prod_{i \in E} \mathcal{W}_i, \quad (35)$$

where the sum is over all possible configurations of the spins on the vertices.

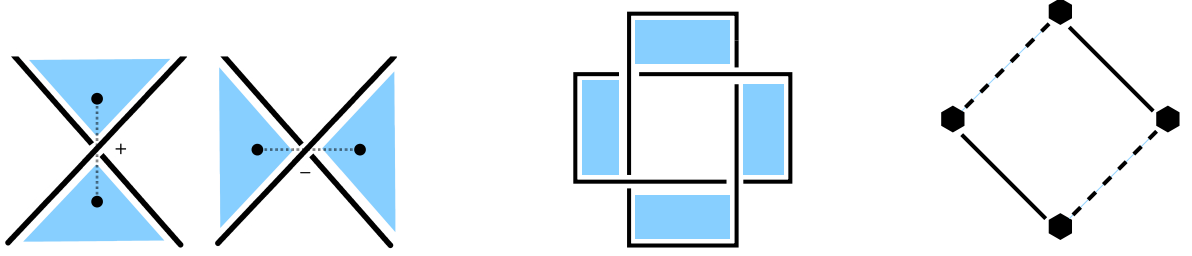


Figure 3: Convention for determining the sign of the edge coupling assigned to each crossing (left). Example of the lattice obtained following the procedure outlined in the text for one of the possible shadings (right). Plain line represent, say, positive couplings, while dashed lines represent negative couplings.

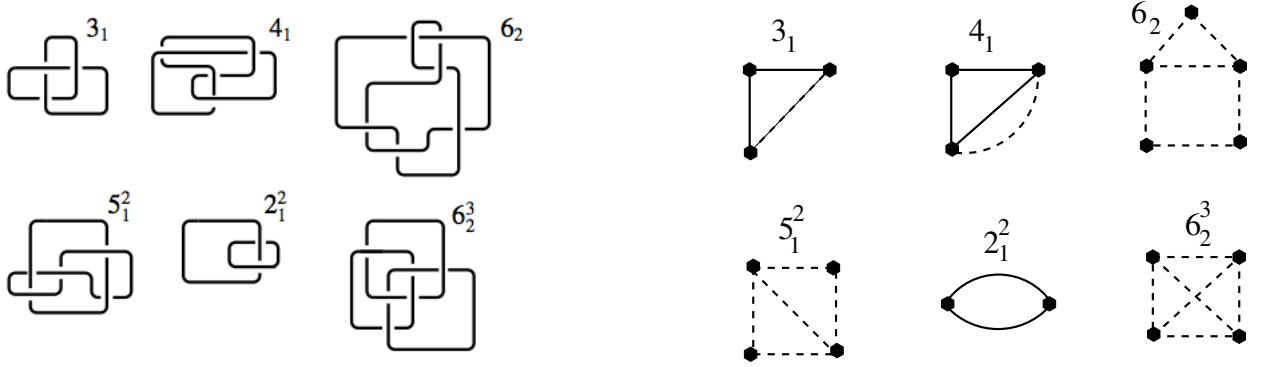


Figure 4: Planar diagrams for some examples of primary knots and links (left) and the associated partition functions (right). Of the two possible graphs for each knot (one for each choice of shading) we have chosen the less trivial one. All the knots lead to statistical mechanics models with nearest neighbor interactions except for the Borromean ring, 6_2^3 .

Z_L is invariant under ambient isotopy provided the weights \mathcal{W}_i satisfy certain conditions, the derivation of which is discussed in [23]. It has been proven that the choice $\mathcal{W}_i^\pm = \exp(\pm\beta\delta_{\sigma,\sigma'})$ where $\sigma = 1, \dots, q$ is compatible with these conditions if

$$\beta = \cosh^{-1} \left(\frac{q-2}{2} \right), \quad (36)$$

holds. In particular, the Potts partition function Z_L for $q = 1, 2$, and 3 at temperatures $\beta = i2\pi/3, i\pi/2$, and $i\pi/3$ respectively is a knot invariant.

We have determined the lattices L for six examples of knots and links (see figure 5) and computed Z_L for a Potts model defined on L with $q = 1, 2$ and 3 for the values of β where the partition function is a knot invariant (see table 1). The invariant corresponding to the value $q = 1, 2$ are actually trivial. The case where $q = 3$ is more interesting. A classical algorithm to compute this invariant exists which works in a time that scales polynomially with the number of crossings [24]. In turn, using a generalisation to three-level systems of the scheme presented in Section 2 allows to estimate the quantum invariant Z_L in *constant* time with an additive error that scales like $1/\sqrt{R}$ where R is the number of repetitions of the experiment, now independent of the number of crossings.

	$q = 1$	$q = 2$	$q = 3$
3_1	$e^{i\frac{5\pi}{6}}$	$4e^{i\frac{5\pi}{8}}$	$\frac{3}{2}(7\sqrt{3} - i)e^{i\frac{1\pi}{4}}$
4_1	$-e^{i\frac{\pi}{3}}$	4	$-\frac{15}{2}(1 - \sqrt{3}i)$
6_2	-1	$-8e^{i\frac{\pi}{4}}$	$3(15 - 22i)$
5_1^2	$-e^{i\frac{5\pi}{6}}$	$8e^{i\frac{3\pi}{8}}$	$\frac{3}{2}(9\sqrt{3} + 29i)e^{i\frac{3\pi}{4}}$
2_1^2	$-e^{i\frac{2\pi}{3}}$	0	$\frac{3}{2}(3 + \sqrt{3}i)$
6_2^3	-1	$8\sqrt{2}$	$-3(9\sqrt{3} + 4i)$

Table 1: Knot invariants computed from the Potts model partition functions defined on the lattices in figure 5. The temperatures at which the partition functions have been evaluated are given in the text.

6 Computational Power of Classical Models

The analysis presented in Section 4 demonstrates how one can sample from a family of quantum circuits with fixed topology in d dimensions to construct a partition function on a classical spin system with fixed topology in $d + 1$ dimensions. One could ask whether the reverse can be done, i.e. given a classical partition function can one then reconstruct the outcomes of a related quantum circuit for a family of coupling parameters? Even more, is it possible that given the ability to compute the partition function of a suitably large classical system and for a suitable set of temperatures, one can reconstruct the outcome of measurements on arbitrary quantum computations of polynomial length in some fixed register input size? This has been partially answered in Ref. [2] where the authors show that the problem of computing the partition function of several classical spin models including the planar Ising model with magnetic fields all with *complex* couplings is BQP-complete. Such classical models do arise for some problems, e.g. the use of the Potts model with complex couplings to compute link invariants as discussed in Sec. 5, but it would be useful to have a result for physical, i.e. *real*, couplings. We do so in this section and also describe some applications: one for investigating quantum phase transitions given the ability to compute classical partition functions, and another for computing partition functions given the ability to prepare and measure corner magnetisation on physically prepared classical thermal states.

6.1 Estimating quantum computations from Ising model partition functions

We show the following:

Theorem 6.1 *Estimation of the partition function $Z(\beta)$ of a two dimensional ferromagnetic, consistent Ising model at inverse temperature β on a square lattice of size $n \times m$ with $m = O(\text{poly}(n))$ with non uniform couplings and magnetic fields with additive error $\delta(n, m, \beta) < \exp(nm(49\beta - 190)/2)$ is BQP-hard, i.e. it is at least as hard as simulating an arbitrary polynomial time quantum algorithm on n qubits. By ferromagnetic we mean the couplings $J_{i,j}$ in Eq. 1 are all positive and by consistent the magnetic fields h_i are all non-negative or all non-positive. To simulate a quantum algorithm means to do the following: For a unitary W built from a quantum circuit composed of $O(\text{poly}(n))$ one and two qubit gates on a length n register provide an estimate of a complex scattering matrix element satisfying*

$$|\langle +_x^{\otimes n} | \widehat{W} | +_x^{\otimes n} \rangle - \langle +_x^{\otimes n} | W | +_x^{\otimes n} \rangle| \leq \frac{1}{O(\text{poly}(n))}$$

with a probability that is exponentially in n close to 1.

Proof:

The proof follows in several stages. First we write an arbitrary polynomial sized quantum circuit in a convenient spatially translationally invariant form. Then we show that the scattering matrix element is equivalent to a complex temperature classical Ising model on a square lattice. Finally, we show that sampling the partition function over many real temperatures of a ferromagnetic Ising model, one can reconstruct the scattering matrix element.

There are many possible equivalent quantum circuits which construct a given unitary. We pick a quantum circuit with a coupling graph given by a one dimensional chain of qubits with open boundaries. In order to perform a universal gate set, one needs a quantum circuit with gates either inhomogeneous in space or time or both. We pick circuits which are homogenous in space only as they are simple to parameterize and it is pedagogically satisfying that each step in the quantum algorithm can be thought of as a Wick rotated transfer matrix generated by a spatially homogenous quantum Hamiltonian. Several models exist for universal quantum computation which use 1D architectures with global interactions [13, 15]. We pick a convenient one due to Raussendorf [14] which involves encoding quantum information in a 1D redundified data register, i.e. the data register is redundified in a second register which is spatially mirrored with respect to the first. This method has the advantage that all gates acting on the system are translationally invariant and the initial state is translationally invariant, e.g. $|+_x^{\otimes n}\rangle$. The only requirements are uniform Ising interactions between nearest neighbours and global single qubit gates. Addressability is afforded by temporal addressing via judiciously chosen homogenous local operations. Readout can be done again using global operations with the assistance of interspersed ancillary qubits or instead by using ancillary levels of each qubit [25]. The overall overhead incurred using global operations in this mirror encoded state is linear in n [14].

Consider a quantum register of an even number n of logical qubits, encoded by a chain of $2n$ qubits. The encoding has a mirror structure, i.e. the wave function of the system is at all times of the form $|\psi\rangle_{1\dots n} \otimes |\psi\rangle_{2n\dots n+1}$. The first ingredient in our proof of the BQP-hardness of the Ising model is the following lemma:

Lemma 6.2 *Let*

$$\sigma_{\text{tot}}^\alpha(\theta) = \prod_{j=1}^{2n} e^{i\frac{\theta}{2}\sigma_j^\alpha}, \quad \alpha = x, y, z, \quad \text{CP}_{\text{tot}} = \prod_{j=1}^{2n-1} \text{CP}_{j,j+1}, \quad \text{Had}_{\text{tot}} = \prod_{j=1}^{2n} \text{Had}_j, \quad (37)$$

denote a set of translationally invariant (global) operations, where $\text{Had} = e^{i\frac{\pi}{2\sqrt{2}}(\sigma_j^x + \sigma_j^z)}$ denotes a single qubit Hadamard gate and $\text{CP} = e^{i\pi|11\rangle\langle 11|}$ the controlled phase gate. The subset

$$\mathfrak{G} = \{\text{CP}_{\text{tot}}, \sigma_{\text{tot}}^z(\pi/8), \text{Had}_{\text{tot}}\} \quad (38)$$

is universal for quantum computation.

Proof: This is proved in Appendix D. □

This lemma implies that for any $\epsilon > 0$, there exists a sequence of operators $\{\mathcal{L}_t \in \mathfrak{G} : t = 0 \dots m-1\}$, such that

$$|\langle +_x^{\otimes n} | \widehat{W} | +_x^{\otimes n} \rangle - \langle +_x^{\otimes 2n} | \prod_{t=0}^{m-1} \mathcal{L}_t | +_x^{\otimes 2n} \rangle| \leq \epsilon, \quad (39)$$

where $m = O(\text{poly}(\log \frac{1}{\epsilon}, n))$. Let σ_{tot} label classical configurations for the $2n$ -qubit chain (element of the computational basis). The action of $\sigma_{\text{tot}}^z(\pi/4)$ and CP_{tot} (up to a global phase) can be expressed as

$$\sigma_{\text{tot}}^z(\pi/8)|\sigma_{\text{tot}}\rangle = e^{i\frac{\pi}{16}\sum_{k=1}^n \sigma_k} |\sigma_{\text{tot}}\rangle, \quad \text{CP}_{\text{tot}}|\sigma_{\text{tot}}\rangle = e^{i\frac{\pi}{4}(\sum_{k=1}^{2n-1}(\sigma_k + \sigma_{k+1}) + \sum_{k=1}^{2n-1} \sigma_k \sigma_{k+1})} |\sigma_{\text{tot}}\rangle, \quad (40)$$

while the matrix elements of a Hadamard gate (up to a global phase) read

$$\langle \sigma | \text{Had} | \sigma' \rangle = \frac{1}{\sqrt{2}} e^{i\frac{\pi}{4}(\sigma+\sigma')} e^{i\frac{\pi}{4}\sigma\sigma'}. \quad (41)$$

These expressions will help us to express the quantum amplitude $\langle +_x^{\otimes 2n} | \prod_{t=0}^{m-1} \mathcal{L}_t | +_x^{\otimes 2n} \rangle$ as an Ising partition function. It is convenient to introduce the following class of operators:

$$\mathcal{T}_s = (\text{CP}_{\text{tot}})^{e_0(s)} (\sigma_{\text{tot}}^z(\pi/8))^{e_1(s)} 2^n \text{Had}_{\text{tot}}^{1-\delta_{s,0}},$$

where the exponents $e_0(s)$ and $e_1(s)$ take values in $\{0, 1\}$. Up to constant factors, it is clear that the operators $\sigma_{\text{tot}}^z(\pi/8)$, Had_{tot} and CP_{tot} can each be expressed either as a single \mathcal{T} -type operator or as a product of at most 2 \mathcal{T} operators. Consequently, we can write

$$\langle +_x^{\otimes 2n} | \prod_{t=0}^{m-1} \mathcal{L}_t | +_x^{\otimes 2n} \rangle = \frac{1}{2^{nM}} \langle +_x^{\otimes 2n} | \prod_{s=0}^{M-1} \mathcal{T}_s | +_x^{\otimes 2n} \rangle, \quad (42)$$

where $M \geq 1$. If $M = 1$ then the overlap is: $\langle +_x^{\otimes 2n} | \prod_{t=0}^{m-1} \mathcal{L}_t | +_x^{\otimes 2n} \rangle = 2^{-n} Z_{1D}(\frac{i\pi}{16})$ where Z_{1D} is the partition function for a classical Ising model in 1D with magnetic fields. Since one dimensional Ising models are exactly solvable for any temperature, including complex temperatures, then so is the overlap. Non exact estimations of scattering matrix element occur for $M > 1$. Since each layer operator \mathcal{L}_t can be expressed as a product of at most two such operators \mathcal{T}_s , we see that M is polynomial in n (since we assume that W is a polynomial depth quantum circuit). This last form of the quantum scattering amplitude, together with the identities (40, 41) allow to express the quantum scattering amplitude as the partition function of an Ising model at imaginary temperature. Up to a global irrelevant phase, we have

$$\langle +_x^{\otimes 2n} | \prod_{t=0}^{m-1} \mathcal{L}_t | +_x^{\otimes 2n} \rangle = \frac{1}{2^{n(M+2)}} \sum_{\{\sigma\}} e^{-\frac{i\pi}{16} H(\sigma)}, \quad (43)$$

where $H(\sigma)$ denotes the Hamiltonian of the form (1), defined on a square $(2n) \times M$ lattice. Simple inspection shows that all couplings (resp. fields) appearing in this Hamiltonian are positive integers, whose magnitude do not exceed 4 (resp. 17).

Let us now assume we are provided with the following resource:

IsingEstimator: Given an inverse temperature, β , and an inhomogeneous Ising Hamiltonian, defined on a two-dimensional square lattice of size $n_x \times n_y$, a device provides an estimate $\hat{Z}(\beta)$ for the partition function, $Z(\beta)$, that satisfies

$$\text{Prob}[|\hat{Z}(\beta) - Z(\beta)| \leq \epsilon \delta(n_x, n_y, \beta)] \geq \frac{3}{4}, \quad (44)$$

in a time that is polynomial in $n_x, n_y, \beta, 1/\epsilon$.

Our goal now is to study how we could design the function δ so that this resource allows for an efficient estimation of scattering amplitudes of quantum circuits. Since all magnetic fields and couplings appearing in the definition of the classical Hamiltonian associated with a quantum circuit are integers, the r.h.s of (43) can certainly be written as

$$\frac{1}{2^{n(M+2)}} \sum_{\{\sigma\}} e^{-\frac{i\pi}{16} H(\{\sigma\})} = \frac{1}{2^{n(M+2)}} \sum_{k=-M'}^{+M'} c_k e^{ik\pi/16},$$

for some coefficients c_k . The value of the integer M' is at most $\max_{\sigma} H(\sigma)$. The r.h.s. of the last equation can equivalently be written as

$$\frac{1}{2^{n(M+2)}} \sum_{\{\sigma\}} e^{-\frac{i\pi}{16} H(\sigma)} = \frac{e^{-iM'\pi/16}}{2^{n(M+2)}} \mathcal{P}(e^{i\pi/16}),$$

where \mathcal{P} is a degree- $(2M')$ polynomial. For all $\beta \geq 0$, our resource allows to compute an estimate $\widehat{\mathcal{P}}(e^{-\beta}) \equiv e^{-\beta M'} \widehat{Z}(\beta)$ for $\mathcal{P}(e^{-\beta})$ that obeys $|\widehat{\mathcal{P}}(e^{-\beta}) - \mathcal{P}(e^{-\beta})| \leq \epsilon e^{-\beta M'} \delta(2n, M, \beta)$. Using a Lagrange polynomial interpolation based on K points $\{(e^{-\beta_j}, \widehat{\mathcal{P}}(e^{-\beta_j})), j = 0 \dots K-1\}$ ($K \geq 2M' + 1$), we re-construct the polynomial \mathcal{P} as

$$\widehat{\mathcal{P}}(z) = \sum_{j=0}^K \widehat{\mathcal{P}}(e^{-\beta_j}) \ell_j(z), \quad \ell_j(z) = \prod_{k \neq j} \frac{z - e^{-\beta_k}}{e^{-\beta_j} - e^{-\beta_k}}, \quad z \in \mathbb{C}.$$

This reconstructed polynomial is in turn used to estimate our quantum amplitude as $\langle +_x^{\otimes 2n} | \prod_{t=0}^{m-1} \mathcal{L}_t | +_x^{\otimes 2n} \rangle_{\text{est}} = \frac{e^{-iM'\pi/16}}{2^{n(M+2)}} \widehat{\mathcal{P}}(e^{i\pi/16})$. The error over this estimate can be bounded as

$$|\langle +_x^{\otimes 2n} | \prod_{t=0}^{m-1} \mathcal{L}_t | +_x^{\otimes 2n} \rangle - \langle +_x^{\otimes 2n} | \prod_{t=0}^{m-1} \mathcal{L}_t | +_x^{\otimes 2n} \rangle_{\text{est}}| \leq \frac{1}{2^{n(M+2)}} \sum_{j=0}^{K-1} \epsilon \delta(2n, M, \beta_j) e^{-M'\beta_j} |\ell_j(e^{i\pi/16})|.$$

It would be desirable to pick the integer K and the temperatures β_j in such a way that the r.h.s. of this last inequality is minimised. Presumably, calculus of variations might make this task doable. We have proceeded in a simpler way and made the choice

$$e^{-\beta_j} = j/K, j = 0 \dots K-1.$$

Then,

$$|\ell_j(e^{i\pi/8})| = \frac{\prod_{k \neq j} |K e^{i\pi/8} - k|}{\prod_{k \neq j} |j - k|}.$$

A closed form for the denominator on the r.h.s. of this expression can be easily worked out:

$$|\prod_{k \neq j} (j - k)| = \prod_{k=0}^{j-1} (j - k) \times \prod_{k=j+1}^{K-1} (k - j) = j! (K - j - 1)!$$

For the numerator, we observe that

$$\prod_{k \neq j} |K e^{i\pi/16} - k| = \frac{K^K}{|K e^{i\pi/16} - j|} \prod_{k=0}^{K-1} |e^{i\pi/16} - k/K| = \frac{K^K}{|K e^{i\pi/16} - j|} \exp \left[\sum_{k=0}^{K-1} \ln \sqrt{(\cos \frac{\pi}{16} - \frac{k}{K})^2 + \sin^2 \frac{\pi}{16}} \right].$$

The argument of the last exponential is:

$$\frac{1}{2} \sum_{k=0}^{K-1} \ln \left[(\cos \frac{\pi}{16} - \frac{k}{K})^2 + \sin^2 \frac{\pi}{16} \right] \times \frac{K}{K} < \frac{K}{2} \int_0^1 \ln \left[(\cos \frac{\pi}{16} - x)^2 + \sin^2 \frac{\pi}{16} \right] dx < -0.744K$$

Plugging these results in our bound for the error on the quantum amplitude, we find that, in the limit of large K ,

$$|\langle +_x^{\otimes 2n} | \prod_{t=0}^{m-1} \mathcal{L}_t | +_x^{\otimes 2n} \rangle - \langle +_x^{\otimes 2n} | \prod_{t=0}^{m-1} \mathcal{L}_t | +_x^{\otimes 2n} \rangle_{\text{est}}| < \frac{\epsilon}{2^{n(M+2)}} \sum_{j=0}^{K-1} \frac{\delta(2n, M, \beta_j) (j/K)^{M'} K^K e^{-0.744K}}{|K e^{i\pi/16} - j| j! (K - j - 1)!}.$$

Considering the case where $K = 2M' + 1$, having an error

$$\delta(2n, M, \beta) \leq \sin \frac{\pi}{16} e^{(\beta+1.488)M'} 2^{n(M+2)} \Gamma((2M' + 1)e^{-\beta} + 1) \Gamma((2M' + 1)(1 - e^{-\beta})) (2M' + 1)^{-2M'}$$

is therefore sufficient for efficient reconstruction of quantum amplitudes. Note that the maximum energies from vertical and horizontal bonds in the lattice is $4(2n(M - 1) + (2n - 1)M)$ and the maximum local field energy is $2n(M - 2)8 + 2n8 + 2nM + 4M((2n - 2)2 + 2)$. Then we have the bound: $M' \leq 50nM - 12M - 24n$. To work out how large $\delta(2n, M, \beta)$ is compared to the partition function, we can compute the needed accuracy for a function of the error $\delta(2n, M, \beta')$ (we use a scaled temperature $\beta' = \beta / \ln 2$ to simplify the expression)

$$f_{\text{error}}(2n, M, \beta') \equiv -\frac{\ln \delta(2n, M, \beta')}{\beta' 2nM} > -\frac{M' \ln 2}{2nM} + \frac{M' \ln 2(0.7387 + 2 \log_2(2M' + 1) - 2 \log_2 M')}{\beta' nM}.$$

For large system sizes,

$$f_{\text{error}}(2n \gg 1, M \gg 1, \beta') > -25 \ln 2 + 50 \ln 2(2.7387)/\beta'.$$

Finally we get a bound for the permissible additive error in the estimation:

$$\delta(2n, M, \beta) < \exp(nM(49\beta - 190)) \quad (45)$$

Writing $n_x = 2n, n_y = M$, since estimating $Z(\beta)$ for a polynomial number (linear in n_y) of temperatures with additive error $\delta(n_x, n_y, \beta)$ on each provides the requisite estimate of the quantum scattering matrix element on a poly(n) sized quantum circuit, the complexity of the estimate of $Z(\beta)$ for an arbitrary temperature is BQP-hard. This completes the proof of Theorem 6.1. \square

We have found how much relative error we can tolerate in an estimation of a classical partition function and still accurately estimate quantum scattering amplitudes. How does this compare to known accuracy of classical algorithms which provide estimates of these partition functions? In Ref. [26] Jerrum and Sinclair construct a fully polynomial randomized approximation scheme (FPRAS) for computing the partition function of an arbitrary classical ferromagnetic Ising model that is consistent. Specifically they provide a classical algorithm that computes an estimate $\hat{Z}(\beta)$ of the partition function $Z(\beta) = \sum_{\{\sigma\}} e^{-\beta H(\{\sigma\})}$ for the ferromagnetic Hamiltonian $H(\{\sigma\})$ on N spins, with a multiplicative error ϵ and success probability

$$\text{Prob} \left[|\hat{Z}(\beta) - Z(\beta)| \leq \epsilon Z(\beta) \right] \geq \frac{3}{4}$$

in a run time polynomial in $N, 1/\epsilon$. This probability of success can be boosted to $1 - \delta$ in a number $\log(1/\delta)$ of repetitions [26]. Since the classical Hamiltonian in Eq. 43 is ferromagnetic, then when $\delta(2n, M, \beta) \geq Z(\beta)$, `IsingEstimator` is no more powerful than FPRAS. In other words, if the tolerable error of `IsingEstimator` could be equal to or greater than $Z(\beta)$ for the relevant temperatures needed to reconstruct the scattering matrix element, then BQP-hard problems can be computed in polynomial time via FPRAS. This is not expected to be the case so we almost certainly have the requirement that the inequality in Eq. 6.1 is $\delta(2n, M, \beta) < Z(\beta)$ over some significant range of temperatures and that it is smaller by an exponential in the problem size M' . Note it is known that the problem of *exactly* computing the partition function for even a ferromagnetic classical Ising model is #P-complete [26]. This complexity class is the same as that for counting the number of satisfying assignments of a Boolean function and counting optimal Traveling Salesman tours. Approximating the partition function with multiplicative error for an anti-ferromagnetic Ising model on a square lattice is NP-hard and for the ferromagnetic model but with general fields is approximation preserving reducible to the complexity class #BIS [27]. The latter is as hard as computing the number of independent sets, (an independent set is a set of vertices that does not contain both endpoints of any edge), in a bipartite graph which is thought to be of intermediate complexity between #P and FPRAS.

6.2 Ising models to compute quantum ground state overlaps

We now consider an application of the mapping between classical partition functions and quantum scattering matrix amplitudes: measuring ground state wavefunction overlaps of quantum Hamiltonians. It has been argued in Ref. [28] that wave function overlaps, termed fidelity overlap, can be a good witness to quantum phase transitions when the ground states straddle a phase transition point. In an ideal laboratory, this problem could be split in two: prepare two quantum registers in the desired states and measure the overlap using, for example, the protocols in Sec. 3. A possibility for the preparation step is to initialise the quantum system in the ground state $|\Psi_0\rangle$ of some simple hamiltonian \hat{H}_0 , and to evolve this Hamiltonian to the target Hamiltonian \hat{H}^* . A fundamental result of quantum mechanics, known as the adiabatic theorem, is that if the Hamiltonian is modified slowly enough, the state obtained at the end of the evolution will be very close to the true ground state $|G\rangle$ [29]. Crucially, the time of the evolution need only grow *polynomially* with the inverse of the minimum gap of the system, γ .

The purpose of this section is to exhibit situations for which the adiabatic evolution need not be actually implemented. We are going to show that, in a precise sense, "time can be replaced with space". Roughly speaking, we are going to show that, instead of performing measurements on a quantum system of a given size, say "size" that has been *evolved* for a time "time", we can equivalently measure partition functions of classical Ising models prepared on a system of size $O(\text{size} \times \text{time})$.

To make things precise, we will focus on the quantum transverse Ising model, described by the Hamiltonian²:

$$\hat{H}^* = -h_\perp \sum_{i \in \Lambda} \sigma_i^x - J \sum_{\langle i, j \rangle \in E(\Lambda)} \sigma_i^z \sigma_j^z - h \sum_{i \in \Lambda} \sigma_i^z, \quad (46)$$

where Λ denotes some d -dimensional lattice, and $E(\Lambda)$ denotes the set of edges of Λ . We are going to view this Hamiltonian as a particular member of a family of time-dependent operators labelled by some time index, t . This family is

$$\hat{H}(t) = \hat{H}_0 + \hat{H}_1(t), \quad t \in [0 : T] \quad (47)$$

where

$$\hat{H}_0 = -h_\perp \sum_{i \in \Lambda} \sigma_i^x, \quad \hat{H}_1(t) = -\frac{t}{T} J \sum_{\langle i, j \rangle \in E(\Lambda)} \sigma_i^z \sigma_j^z - \frac{t}{T} h \sum_{i \in \Lambda} \sigma_i^z. \quad (48)$$

Without loss of generality, we will assume that $h_\perp > 0$. In that case, $|\Phi_0\rangle \equiv |+_x^{\otimes |\Lambda|}\rangle$ is of course the (unique) ground state of \hat{H}_0 . Evidently, $\hat{H}(T) = \hat{H}^*$. The starting point of our construction is a discretisation of an adiabatic evolution

Theorem 6.3 *Let T satisfy the inequality*

$$T \geq T_*(\hat{H}, \delta) = \frac{10^5}{\delta^2} \frac{(|h| \cdot |\Lambda| + |J| \cdot |E(\Lambda)|)^3}{\gamma^4}, \quad (49)$$

where $\gamma = \min_{t \in [0: T]} \text{gap } \hat{H}(t)$, where $\text{gap } \hat{H}(t)$ denotes the difference between the two lowest eigenvalues of $\hat{H}(t)$. Let L denote a positive integer, and let us define the discretisation step as

$$\tau \equiv T/L. \quad (50)$$

The quantity by which the state $U_{L-1} U_{L-2} \dots U_0 |+_x^{\otimes |\Lambda|}\rangle$ deviates from the true ground state $|G\rangle$ of H^* is at most

$$\Delta = \delta + T \sqrt{\frac{2(|h| \cdot |\Lambda| + |J| \cdot |E(\Lambda)|)}{L}} + KL(|h| \cdot |\Lambda| + |J| \cdot |E(\Lambda)|) \cdot |h_\perp| \cdot |\Lambda| \tau^2, \quad (51)$$

²We use the hat on the operator to emphasise that this is a quantum Hamiltonian.

where K is some constant. Each unitary U_k is defined as

$$U_k = e^{-i\tau\hat{H}_0} e^{-i\tau\hat{H}_1(k\tau)}. \quad (52)$$

This theorem, whose proof is given in Appendix F, will help us to study fidelity overlaps,

$$f = \langle \tilde{G} | G \rangle,$$

where $|G\rangle$ is the ground state of \hat{H}^* and $|\tilde{G}\rangle$ is the ground state of some other Hamiltonian $\hat{\tilde{H}}^*$. For $T(T')$ and $L(L')$ large enough to build an approximation to $|G\rangle(|\tilde{G}\rangle)$, f can be replaced in good approximation with

$$f \simeq \langle +_x^{\otimes |\Lambda|} | W_0^\dagger W_1^\dagger \dots W_{L'-1}^\dagger U_{L-1} U_{L-2} \dots U_0 | +_x^{\otimes |\Lambda|} \rangle. \quad (53)$$

For the transverse Ising model exemplified here the fidelity estimate which gives witness to a quantum phase transition is for the case $|G\rangle$ being the ground state of \hat{H}^* with couplings $h = 0$ and $|\tilde{G}\rangle$ being the ground state of $\hat{\tilde{H}}^*$ with couplings $h' = 0$, $J' = J$, and $h'_\perp = h_\perp + \delta h_\perp$. Near the critical point, $h_\perp = J$, there is a strong dip in the fidelity especially pronounced for $\delta_\perp h/J \sim 0.2$ [30].

We are going to use a classical argument of quantum field theory [31], in a simple form adapted to our purposes, and show that the overlap (53) can be expressed as a partition function for a $d + 1$ -dimensional many body system at finite (complex) temperature, described by a suitable *classical* Ising Hamiltonian. The operator $e^{-i\tau\hat{H}_0}$ can be expressed as the transfer matrix of a *classical* system, using the identity [32]

$$T(\beta) = \sum_{\sigma\sigma'} e^{\beta\sigma\sigma'} |\sigma\rangle\langle\sigma'| = e^\beta (\mathbf{1} + e^{-2\beta}\sigma^x). \quad (54)$$

Since on the other hand,

$$e^{-i\tau h_\perp \sigma^x} = \cos(\tau h_\perp) (\mathbf{1} - i \tan(\tau h_\perp) \sigma^x),$$

it would be natural to make the identification $e^{-2\beta} = -i \tan \tau h_\perp$, giving $\beta = i\frac{\pi}{4} - \frac{1}{2} \ln \tan(\tau h_\perp)$, in order to relate $\gamma_{r_1 r_2}$ to a classical model. Rather we are going to express the single-site unitary operator $e^{-i\tau h_\perp \sigma^x}$ in terms of *two* operators T . For $\epsilon > 0$, let us define $\beta_\pm(\epsilon)$ through

$$e^{-2\beta_\pm(\epsilon)} = \mp i(1 \pm \epsilon). \quad (55)$$

One checks that

$$T(\beta_+(\epsilon)) T(\beta_-(\epsilon)) = (2 - \epsilon^2) e^{(\beta_+(\epsilon) + \beta_-(\epsilon))} [\mathbf{1} - i \frac{2\epsilon}{2 - \epsilon^2} \sigma^x]. \quad (56)$$

This choice of using two transfer matrices is not strictly necessary but it guarantees that the amount by which β_+ and β_- need deviate from the imaginary axis is small which makes the connection to the traditional classical to quantum mappings [31] more transparent.

So, for

$$\frac{2\epsilon}{2 - \epsilon^2} = \tan(\tau h_\perp), \quad (57)$$

we see that the operator $e^{-i\tau\hat{H}_0}$ can be expressed as a product of two *classical* Ising transfer matrices:

$$e^{-i\tau\hat{H}_0} = \left[\sqrt{\frac{1 - \epsilon^2}{\epsilon^4 + 4}} \right]^{|\Lambda|} \prod_{x \in \Lambda} T_x(\beta_+(\epsilon)) \prod_{y \in \Lambda} T_y(\beta_-(\epsilon)).$$

This latter identity allows to express each operator U_k in terms of classical Ising transfer matrices. Introducing closure relations and bearing in mind that the operator $\hat{H}_1(t)$ is diagonal in computational basis,

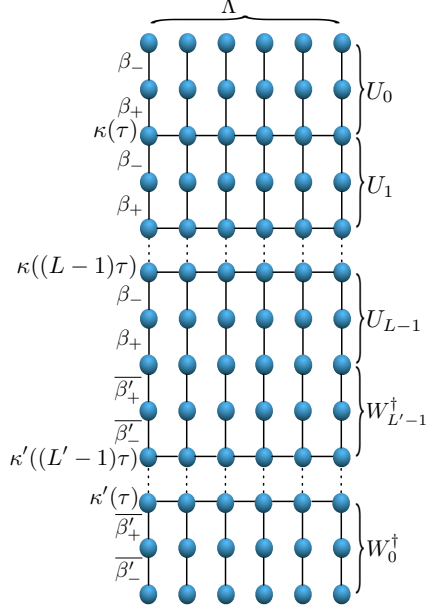


Figure 5: Representation of the $d + 1$ dimensional classical Ising spin lattice with couplings that encode information of the wavefunction overlap on a d dimensional quantum spin lattice Λ . Here the overlap is $\langle \tilde{\Psi}^* | \Psi^* \rangle$ which is an approximation to the fidelity $f = \langle \tilde{G} | G \rangle$, where $|G\rangle$ is the ground state of a Hamiltonian \hat{H} and $|\tilde{G}\rangle$ is the ground state of \hat{H}^* . The sequence $U_{L-1} \dots U_0$ provides for adiabatic evolution, in small time steps τ , of a time dependent Hamiltonian $\hat{H}(t)$ from the product state $|+_x^{\otimes |\Lambda|}\rangle$ to $|\Psi^*\rangle$ (which is an approximation to $|G\rangle$), and similarly for the sequence $W_{L-1}^\dagger \dots W_0^\dagger$, in steps τ' , which builds an approximation $|\tilde{\Psi}^*\rangle$ of $|\tilde{G}\rangle$ from $|+_x^{\otimes |\Lambda|}\rangle$. Note that the number of gates L and L' to reach target ground states could differ as will the couplings generically. Each gate is a composition of diagonal gates with dimensionless coupling $\kappa(t)$ and two non diagonal gates with dimensionless couplings β_\pm . The temporal evolution of quantum gates can be represent on a classical spin lattice of one extra dimension with bond couplings as indicated on the left. For the Hamiltonian in Eq. 47 $\kappa(k\tau)$ means dimensionless row couplings βk between nearest neighbour spins, local fields of strength $\beta k h / J$, and couplings β_\pm between rows. The parameters for adiabatic evolution to $|\tilde{\Psi}^*\rangle$ are indicated with primes.

the matrix elements of each operator U_k can now be expressed as a sum over paths on three copies of the lattice Λ :

$$U_k = \sum_{\sigma(k)} \sum_{\sigma(k+1)} \sum_{\sigma(k+2)} e^{\mathcal{L}_{\sigma(k), \sigma(k+1), \sigma(k+2)}} |\sigma(k+2)\rangle \langle \sigma(k)|,$$

Here $\sigma(k)$ denotes a classical spin configurations over one copy of Λ , and the interaction \mathcal{L} , defined over a lattice $\Lambda \times \Lambda \times \Lambda$, is

$$\mathcal{L}_{\sigma(k), \sigma(k+1), \sigma(k+2)} = \beta_- \sum_{j \in \Lambda} \sigma_j(k) \sigma_j(k+1) + \beta_+ \sum_{j \in \Lambda} \sigma_j(k+1) \sigma_j(k+2) - i \frac{k\tau^2}{T} \left(J \sum_{\langle i, j \rangle \in E(\Lambda)} \sigma_i(k) \sigma_j(k) + h \sum_{j \in \Lambda} \sigma_j(k) \right).$$

This interaction looks like a classical spin interaction with alternating complex couplings β_+, β_- in the “time” direction which transfers between different copies of the lattice Λ and complex coupling within the lattice Λ . We would like to be able to chose variable couplings along the “space” and “time” directions so

we define a new interaction (assuming $J \neq 0$)

$$\mathcal{H}_{\sigma(k),\sigma(k+1),\sigma(k+2)} = \beta_- \sum_{j \in \Lambda} \sigma_j(k) \sigma_j(k+1) + \beta_+ \sum_{j \in \Lambda} \sigma_j(k+1) \sigma_j(k+2) + \beta k (\sum_{\langle i,j \rangle \in E(\Lambda)} \sigma_i(k) \sigma_j(k) + \frac{h}{J} \sum_{j \in \Lambda} \sigma_j(k)).$$

A similar Hamiltonian can be written to represent evolution by gates W_k^\dagger :

$$\mathcal{H}'_{\sigma(k),\sigma(k+1),\sigma(k+2)} = \beta'_+ \sum_{j \in \Lambda} \sigma_j(k) \sigma_j(k+1) + \beta'_- \sum_{j \in \Lambda} \sigma_j(k+1) \sigma_j(k+2) + \beta' (L' + L - 1 - k) (\sum_{\langle i,j \rangle \in E(\Lambda)} \sigma_i(k+3) \sigma_j(k+3) + \frac{h'}{J'} \sum_{j \in \Lambda} \sigma_j(k+3)).$$

Now we can write a Hamiltonian on the *enlarged* lattice $\hat{\Lambda} = \{1, \dots, 2(L + L') + 1\} \times \Lambda$,

$$-H(\{\sigma\}) = \sum_{k=0}^{L-1} \mathcal{H}_{\sigma(2k+1),\sigma(2k+2),\sigma(2k+3)} + \sum_{k=L}^{L'+L-1} \mathcal{H}'_{\sigma(2k+1),\sigma(2k+2),\sigma(2k+3)},$$

which takes exactly the form of a classical $(d+1)$ -dimensional Ising Hamiltonian but with complex couplings. The associated partition function depends on the vector of couplings $\vec{\beta} \equiv \{\beta_+, \beta_-, \beta'_+, \beta'_-, \beta, \beta'\}$

$$Z(\vec{\beta}) = \sum_{\{\sigma\}} e^{-H(\{\sigma\})}$$

and is a sum over classical configurations defined over $\hat{\Lambda}$.

Substituting this expression in Eq.(53), we see that the fidelity overlap can be approximated by

$$f = \frac{1}{2^{|\Lambda|}} \left[\sqrt{\frac{1-\epsilon'^2}{\epsilon'^4+4}} \right]^{L|\Lambda|} \left[\sqrt{\frac{1-\epsilon'^2}{\epsilon'^4+4}} \right]^{L'|\Lambda|} Z(\vec{\beta}^*). \quad (58)$$

where, ϵ' is a solution to $2\epsilon'/(2-\epsilon'^2) = \tan(\tau' h'_\perp)$ appropriate for the quantum Hamiltonian \hat{H}^* and the vector of complex variables $\vec{\beta}^* \equiv \{\beta_+^*, \beta_-^*, \beta'^*_+, \beta'^*_- , \beta^*, \beta'^*\}$ is

$$\begin{aligned} \beta_\pm^* &= \pm \left(\frac{i\pi}{4} + \frac{1}{2} \log \left(1 \pm \left(\sqrt{3 - \cos(2\tau h_\perp)} \csc(\tau h_\perp) / \sqrt{2} - \cot(\tau h_\perp) \right) \right) \right) \\ \beta'^*_\pm &= \mp \left(\frac{i\pi}{4} + \frac{1}{2} \log \left(1 \pm \left(\sqrt{3 - \cos(2\tau' h'_\perp)} \csc(\tau' h'_\perp) / \sqrt{2} - \cot(\tau' h'_\perp) \right) \right) \right) \\ \beta^* &= \frac{iJT}{L^2} \\ \beta'^* &= -\frac{iJ'T'}{L'^2}, \end{aligned} \quad (59)$$

which were obtained by solving Eqs. 55,57. Note for $\tau h_\perp \ll 1$, $\beta_\pm^* = \pm i\frac{\pi}{4} \pm \frac{\tau h_\perp}{2} - O(\tau^2 h_\perp^2)$. which is the statement that the analytic continuation is performed to nearly purely imaginary couplings strengths along the “time” direction.

As described in Sec. 4 we can write the partition function in a power series in exponentials of the coupling parameters. For simplicity we assume $J = J' = 1$, $h' = h = 0$ in which case:

$$Z(\vec{\beta}) = \sum_{g_1=-m_1}^{m_1} \sum_{g_2=-m_2}^{m_2} \sum_{g_3=-m_3}^{m_3} \sum_{g_4=-m_4}^{m_4} \sum_{g_5=-m_5}^{m_5} \sum_{g_6=-m_6}^{m_6} c_{g_1,g_2,g_3,g_4,g_5,g_6} e^{\beta g_1} e^{\beta' g_2} e^{\beta_+ g_3} e^{\beta_- g_4} e^{\beta'_+ g_5} e^{\beta'_- g_6}, \quad (60)$$

where:

$$m_1 = m_2 = L|\Lambda|, \quad m_3 = m_4 = L'|\Lambda|, \quad m_5 = L(L-1)(|\Lambda|-1)/2, \quad m_6 = L'(L'-1)(|\Lambda|-1)/2.$$

In Appendix G it is shown how the coefficients $c_{g_1, g_2, g_3, g_4, g_5, g_6}$ can be obtained by sampling the partition function for $O(\text{poly}(L^2|\Lambda|, L'^2|\Lambda|))$ number of *real* coupling strengths $\vec{\beta}$ which then gives an estimate $\widehat{Z}(\vec{\beta})$. In order to obtain an estimate \hat{f} of the fidelity overlap, we then need to perform an analytic continuation:

$$\hat{f} = \frac{1}{2^{|\Lambda|}} \left[\sqrt{\frac{1-\epsilon^2}{\epsilon^4+4}} \right]^{L|\Lambda|} \left[\sqrt{\frac{1-\epsilon'^2}{\epsilon'^4+4}} \right]^{L'|\Lambda|} \widehat{Z}(\vec{\beta}^*). \quad (61)$$

Suppose we demand the error in the estimation of the fidelity to be $\epsilon = O(1/\text{poly}(|\Lambda|))$:

$$|\hat{f} - f| \leq \epsilon,$$

and that the additive error in the estimation of the classical partition function satisfies

$$\text{Prob}[|\widehat{Z}(\vec{\beta}) - Z(\vec{\beta})| \leq \epsilon \delta(\vec{\beta})] \geq \frac{3}{4}. \quad (62)$$

Then it is shown in Appendix G that the following precision will suffice:

$$\delta(\vec{\beta}) \leq 16(JT)(J'T')L(L-1)L'(L'-1)|\Lambda|^6 e^{(\beta_+ + \beta_- - 6.4)L|\Lambda|} e^{(\beta'_+ + \beta'_- - 6.4)L'|\Lambda|} e^{(\frac{\beta}{2} - 1.6)L(L-1)(|\Lambda|-1)} e^{(\frac{\beta'}{2} - 1.6)L'(L'-1)(|\Lambda|-1)}. \quad (63)$$

To summarize, the required precision in the partition function estimation shows an exponential dependence on quadratic and cubic quantities in the system size. The origin of this dependence lies on the number of Fourier frequencies needed to reconstruct the partition function. This number is obtained by summing the amplitude of the bonds in the lattice (represented in Fig. 5) associated with each coupling. The interactions corresponding to vertical (horizontal) bonds need a number of Fourier frequencies which is quadratic (cubic) in the system size. This different behaviour ultimately comes from the chosen adiabatic time dependence on the total Hamiltonian of the system (Eq. 47).

We close this section by commenting that while fidelity overlaps could be estimated using the method of mapping to a generic quantum circuit presented in Sec. 6.1, the method described here is much more efficient in resource scaling since the gates are applied directly using the transfer matrix formalism rather than mapping to a fixed library of quantum gate in an encoded circuit. Furthermore, the required accuracy of estimation of the partition function is exponentially better than the bound computed in that case (Eq. 45).

6.3 Corner magnetisation and estimating partition functions

The foregoing analysis illustrates the computational power of accurate evaluation of Ising partition functions. We can wonder what is the computational power of more modest tasks, such as estimating the mean values of specific observables. We have studied a simple instance of this problem. As it turns out, very simple tasks already have computational power. For instance, the ability to accurately estimate single site magnetisations on random Ising models lead to random approximation schemes for partition functions. This is the content of the following theorem.

Theorem 6.4 *Consider the Ising model on a two-dimensional square lattice Λ , described by the Hamiltonian:*

$$H(\sigma) = -J \sum_{\langle i, j \rangle} \sigma_i \sigma_j - h \sum_{i \in \Lambda} \sigma_i. \quad (64)$$

For any ϵ , inverse temperature β , and magnetic field strength h it is possible to provide an estimate $\hat{Z}(\beta, h)$ for the Ising partition function $Z(\beta, h)$ satisfying

$$\text{Prob}[|\hat{Z}(\beta, h) - Z(\beta, h)| \leq \epsilon Z(\beta, h)] \geq 3/4, \quad (65)$$

in a time that scales at most polynomially with $\beta, \epsilon^{-1}, |h|$, and the size of the system if we are able to perform corner magnetisation measurements on specific non-homogeneous Ising systems with a relative precision that need not be lower than the inverse of some polynomial in $|h|, \epsilon^{-1}$ and the size of the system.

Proof: The proof is given in Appendix E. □

This result might appear surprising since it applies to even to antiferromagnetic Ising models whereas, as discussed above, a multiplicative approximation of the partition function in that case is an NP-hard problem. However, corner measurement is a quantum process which assumes the thermal state of the classical Hamiltonian has been prepared. Some recent work [20, 34] provides quantum algorithms to simulate thermal states of classical spin models. However as mentioned in Sec. 4, generically these algorithms scale exponentially in the system size, and given the complexity of multiplicative approximations of antiferromagnetic partition functions we would not expect a drastic improvement in thermal state preparation by quantum algorithms in that case. Whether efficient quantum algorithms exist for preparing ferromagnetic thermal states is as far as we know an open problem but if so than corner magnetisation measurement could prove a useful diagnostic for such algorithms since classical FPRAS is available. Finally, we add that recently quantum algorithms for FPRAS were found which exhibit a quadratic speed up over the classical counterparts [35]. These algorithms are rather different in spirit from measuring corner magnetisation as instead of using mixed states they use a combination of Grover search and phase estimation to prepare pure states of many qubit systems which coherently encode probability distributions of various classical spin configurations.

7 Conclusions

In conclusion, we have presented schemes allowing for the measurement of partition functions and mean values of classical many-body systems, at complex temperatures. Although we have mainly focused on Ising Hamiltonians, these schemes can be generalised to other systems, such as the q -state Potts model for instance. We have presented two applications of these schemes.

First, we have studied the possibility to use it in order to compute real temperature partition functions. Although our findings yielded results as poor as previous attempts made by other authors, it is interesting to have found similar results using a different route, in particular one that involves reconstructing partition functions for all temperatures as opposed to a single temperature. We have also seen how experimental data allow to *a posteriori* sharpen error estimates, through a central-limit theorem. To the best of our knowledge, the problem of determining whether quantum mechanics can be used (or not) to efficiently compute partition functions of classical models, or even FPRAS thereof, is still open. As a second application, we have seen how some link invariants could be deduced from the ability to detect imaginary temperature partition functions, again using constant depth quantum circuits.

These applications all rely on two kinds of schemes, one whose implementation could, in principle, only require a constant time, another involving a time evolution. All schemes translate naturally into global operations and measurements supplemented by edge addressability. This is natural for certain architectures such as cold trapped atoms in optical lattices [36], or superconducting qubit arrays [37]. Furthermore, this kind of quantum processing can be made fault tolerant without demanding more addressability as shown in [38].

We have considered the dual of the first application mentioned, and studied the possibility to efficiently simulate a quantum computer, given the ability to estimate *real temperature* disordered Ising partition functions. We have found that quantum amplitude of a depth- D quantum circuit, acting on n qubits, could be reliably estimated if suitably associated disordered Ising models could be evaluated with a precision that essentially grows exponentially with D and n . The problem of simulating quantum circuits from statistical mechanical partition functions, estimated with a looser precision (polynomial, say) is, just as open its dual. One implication is that given the power to compute classical partition functions in $d + 1$ dimensions, in certain cases one can compute quantities relevant to quantum phase transitions in d dimensions. This argument involved viewing the overlap of two ground states of a quantum Hamiltonian as the scattering matrix element for a quantum computation which can then be estimated by computing classical Ising model partition functions with real couplings. The method was illustrated for the particular case of the quantum transverse Ising model in one dimension and while that model, the mapping extends to a variety of other quantum spin Hamiltonians in a straightforward manner. For the sake of simplicity, we have restricted our analysis to some homogeneous quantum Ising models in d dimensions and that model already has a well known correspondence to the $d + 1$ dimensional classical Ising model [23]. However, extensions of our ideas to disordered quantum spin Hamiltonians of the form, say, $\hat{H} = -\sum_i (h_i^x \sigma_i^x + h_i^y \sigma_i^y + h_i^z \sigma_i^z) - \sum_{\langle i,j \rangle} (J_{i,j}^x \sigma_i^x \sigma_j^x + J_{i,j}^y \sigma_i^y \sigma_j^y + J_{i,j}^z \sigma_i^z \sigma_j^z)$ is straightforward.³ This mapping could provide new ways to perform quantum simulation, via either quantum or classical algorithms for estimating Ising model partition functions. Given some of the difficulties that beset fault tolerant implementations of quantum simulations [39, 40] new approaches are certainly desirable.

Finally, we have seen how the ability to prepare thermal states and perform single qubit measurements immediately implies the existence random approximation schemes. This observation naturally leads to wonder what is the quantum complexity of the preparation of classical thermal state. In view of recent inapproximability results [41], it would be very interesting to solve this question in the case of the anti-ferromagnetic Ising model for instance.

8 Acknowledgements

We would like to thank A. Riera, M. Bremner, T. Cubitt, G. De Las Cuevas, J.I. Latorre, D. Pérez-García, J. Twamley, and M. van den Nest for discussions. S.I. acknowledges financial support from the Ramon y Cajal program (RYC-2009-04318). G.K.B. received support from the European Community's Seventh Framework Programme (FP/2007-2013) under grant agreement no. 247687 (Integrating Project AQUITE). G.K.B., M.C., and J.T. received support through the ARC via the Centre of Excellence in Engineered Quantum Systems (EQuS), project number CE110001013.

A Disordered Systems

Preliminary: We found it convenient to use a slight variation of the detection schemes described in Section 2 and consider single qubit gates defined from two Hadamard gates and a single phase gate:

$$G(\theta) = \text{Had} \begin{pmatrix} 1 & 0 \\ 0 & e^{i\theta} \end{pmatrix} \text{Had} . \quad (66)$$

For $\theta^* = -i \log \tanh \beta J$, this single qubit gate turns out to be equal to $T(\beta J)/2 \cosh(\beta J)$, where $T(\beta J)$ is the two-spin Ising transfer matrix introduced in Eq.(54).

³Again, one could use the Baker-Campbell to decompose the evolution operator associated with this Hamiltonian. Then, it would be enough to express σ^y in terms of σ^x and σ^z operators using an Euler angles decomposition.

In this appendix, we are interested in two-dimensional Ising models, of size $n \times m$, with random bond interactions, which strengths take value in $\{-1, +1\}$. The magnetic fields felt by each spin is also assumed to be random and takes value in $\{-1, 0, +1\}$. For a *fixed* configuration of bonds and magnetic fields, the partition function can be evaluated for a specific range of complex temperature, with the help of a two-dimensional lattice of quantum particles on which instantaneous measurements are made, or through the time evolution of a one-dimensional quantum system.

The one-step protocol doesn't pose any particular problem for disordered systems. From quantum amplitudes of the form given by Eq.(7) evaluated at specific angles, one can reconstruct the partition function through analytic continuation. Namely,

$$Z(\beta) = A(i\beta) = \sum_{j_1=0}^{2N_1} w^{(N_1)}(i\beta - \alpha_{j_1}) A\left(\frac{2j_1\pi}{N_1}\right), \quad (67)$$

where $w^{(N_1)}$ is defined by Eq.(26), and where N_1 is polynomial in n and in m .

The case of the time evolved scheme is slightly more complicated than in Section 2. Reproducing the reasoning presented in that section, one can find an appropriate sequence of controlled phase gates (3) and G -gates that provides relevant quantum amplitudes. The real partition functions are again obtained after Fourier transform and analytic continuation. It turns out that three parameters are enough for that. One, α , takes into account constant-time interactions and magnetic fields. The two others, θ^+ and θ^- , are respectively related to ferromagnetic and antiferromagnetic interactions between particles corresponding to consecutive time-slices. More precisely, one can see that the kind of partition functions we wish to consider can be written as

$$Z(\beta) = 2^m (e^\beta + e^{-\beta})^{N_2^+ + N_2^-} \sum_{\nu_1=-N_1}^{N_1} \sum_{\nu_2^+=0}^{N_2^+} \sum_{\nu_2^-=0}^{N_2^-} c_{\nu_1 \nu_2^+ \nu_2^-} e^{\nu_1 \beta (\tanh \beta)^{\nu_2^+ + \nu_2^-}}, \quad (68)$$

where N_1, N_2^+, N_2^- are again polynomial in n and in m . Actually, $N_1 = 2nm - n$ represents a bound on the total number of "horizontal" bonds plus the number of sites, while N_2^+ (resp. N_2^-) represents the number of ferromagnetic (resp. antiferromagnetic) edges connecting spins at different time-slices ("vertical" bonds) ($N_2^+ + N_2^- = m(n-1)$). The coefficients $c_{\nu_1 \nu_2^+ \nu_2^-}$ are essentially Fourier transforms of quantum amplitudes $A(\alpha, \theta^+, \theta^-)$ detected at selected angles $\alpha, \theta^+, \theta^- \in (0, 2\pi]$:

$$c_{\nu_1 \nu_2^+ \nu_2^-} = (-1)^{\nu_2^-} \sum_{j_1=0}^{2N_1} \sum_{j_2^+=0}^{N_2^+} \sum_{j_2^-=0}^{N_2^-} \frac{e^{-2\pi i (\frac{\nu_1 j_1}{2N_1+1} + \frac{\nu_2^+ j_2^+}{N_2^++1} + \frac{\nu_2^- j_2^-}{N_2^-+1})}}{(2N_1+1)(N_2^++1)(N_2^-+1)} A\left(\frac{2j_1\pi}{2N_1+1}, \frac{2j_2^+\pi}{N_2^++1}, \frac{2j_2^-\pi}{N_2^-+1}\right). \quad (69)$$

One can note how the particular form of the G -gate (which does not involve terms of the form $e^{-i\theta}$) allows for the Fourier transform in θ^\pm to be restricted to positive frequencies. Again, plugging Eq.(69) into Eq.(68) allows to express the partition function as a function of the "experimental" data:

$$Z(\beta) = \frac{2^m (e^\beta + e^{-\beta})^{N_2^+ + N_2^-}}{(2N_1+1)(N_2^++1)(N_2^-+1)} \sum_{j_1=0}^{2N_1} \sum_{j_2^+=0}^{N_2^+} \sum_{j_2^-=0}^{N_2^-} A(j_1, j_2^+, j_2^-) \\ (e^\beta e^{-\frac{2i\pi j_1}{2N_1+1}})^{-N_1} S^{(2N_1)}(e^\beta e^{-\frac{2i\pi j_1}{2N_1+1}}) S^{(N)}\left(\tanh \beta e^{-\frac{2i\pi j_2^+}{N_2^++1}}\right) S^{(N)}\left(-\tanh \beta e^{-\frac{2i\pi j_2^-}{N_2^-+1}}\right), \quad (70)$$

where $S^{(N)}(q) \equiv (1 - q^{N+1})/(1 - q)$.

The restricted set of possible values for the couplings and magnetic fields implies that the partition function of the disordered Ising model we are considering can be written as

$$Z(\beta) = \sum_{k=-N}^N \xi_k e^{-k\beta} \quad (71)$$

where again N scales polynomially with the system size, and where each ξ_k is positive integer whose magnitude is at most equal to the number of possible configurations for the system, i.e. $\xi_k \leq 2^{nm}, \forall k$, i.e. they can be represented exactly with nm bits. Thus, the estimation of each coefficient ξ_k with nm bits of accuracy, i.e. with a variance $E_2(\xi_k)$ lower than one would allow for an exact reconstruction of the partition function for *all* temperature. Yet another Fourier transform allows to show that

$$\xi_k = \frac{1}{2N+1} \sum_{j=0}^{2N+1} Z(i \frac{2j\pi}{2N+1}) e^{-i \frac{2j\pi}{2N+1} k}. \quad (72)$$

Combining this latter relation with Eq.(67) for instance, it is possible to see that in order to get ξ_k with nm bits of accuracy, one would need to estimate the quantum amplitudes themselves with $O(nm)$ bits of accuracy. Unfortunately, we do not know how to do that efficiently. In our scheme, the quantum amplitudes are obtained from repeated Bernoulli trials. It therefore seems that $O(2^{nm})$ trials are then necessary. A similar conclusion is reached when the evolution protocol is used.

We now give some more qualitative insight on the performance of the protocol by analyzing a particular instance of the reconstruction (through the time evolving algorithm) of the coefficients ξ_k (Eq. 71) for an 8×8 Ising model with 50% positive/negative bonds and uniform magnetic field (set to 1). In Fig. 6 we plot the coefficients ξ_k together with an upper bound on their standard deviation as a function of k .

We remark that, for small temperatures, only coefficients ξ_k with big k are important as it is evident from the series in Eq. 71. As shown in the plot, in the “big k ” range, two facts are evident: the standard deviation goes to zero and the coefficients ξ_k are exactly zero. The reason behind the behaviour of the standard deviation is found by algebraically expanding equation 68 and noticing that the coefficients (responsible for the amplification the experimental errors) multiplying big powers of e^β are small. On the other hand, the behaviour of the coefficients ξ_k for big k is a natural feature of the disordered model consider here. More specifically, it simply reflects the impossibility for the ground state spin configuration to minimize each local term of the hamiltonian, namely, to satisfy each bond and align to the magnetic field everywhere. The low temperature properties of the model are then shifted around the k s where the coefficients ξ_k start to be non-zero. Unfortunately, in that regime, the error is not longer approaching zero, explaining why, in this case, the protocol does not give good low temperature performances. Conversely, for a uniform ising model, the coefficient ξ_k would be nonzero for the biggest possible k explaining how, in the main text (see Fig. 2) we could get good results in the low temperature limit for this uniform case.

Again by simply inspecting Eq. 71 one can easily get convinced that the importance of the coefficients ξ_k for smaller k becomes more important as the temperature increases. In this regime, the standard deviation is basically constant witnessing properties of the counting process needed to calculate the coefficients ξ_k , again obtained by expanding eq 68 in powers of e^β . As one can infer by the plot, the relative error is quite small for these intermediate values of k , justifying the better high temperatures performances of the protocol.

At last, we would like to qualitatively analyze the possibility to use the protocol to estimate an upper bound of the ground state energy. This relies on restating the problem of finding the ground state energy as the problem of finding the maximum k for which $\xi_k \neq 0$. Following this statement, in order to find an estimate for the upper bound for the ground state energy, we want, roughly speaking, to look at the condition by which the standard deviation on the coefficients ξ_k is not bigger than the coefficients themselves. In the

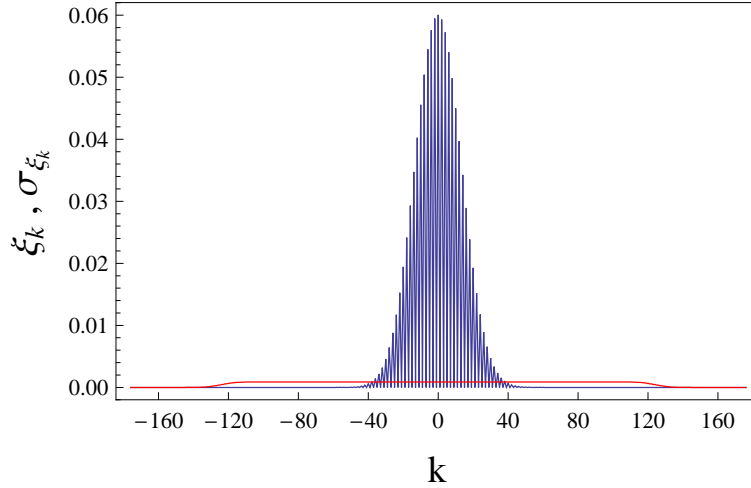


Figure 6: (color online) Plot of the coefficients ξ_k (in blue, see Eq. 71) and an upper bound on their standard deviation σ_{ξ_k} (in red) as a function of k for an 8×8 Ising model with 50% positive/negative bonds and uniform magnetic field (set to 1). From this plot we can qualitatively justify the performances of the algorithm in the small and high temperature limits. The low temperature limit behaviour has to be found in the range of k where the coefficients ξ_k start to be non-zero. This range does not correspond to the maximum possible value of k due to the fact that, in the present model, spin configurations cannot minimize each local hamiltonian. This does not allow to take advantage of the enhanced precision of the protocol for big k and it is the reason for the poor performances of the algorithm at small temperatures. As the temperature increases, the whole range of k starts to become important, so that we can focus on the intermediate values of k , where the bigger coefficients ξ_k are. As evident from the plot, in this regime the relative error is quite small explaining the good high temperatures performances of the protocol. The value of k where the standard deviation is equal to the relative coefficient ξ_k sets the limit for a possible estimate of an upper bound on the ground state energy.

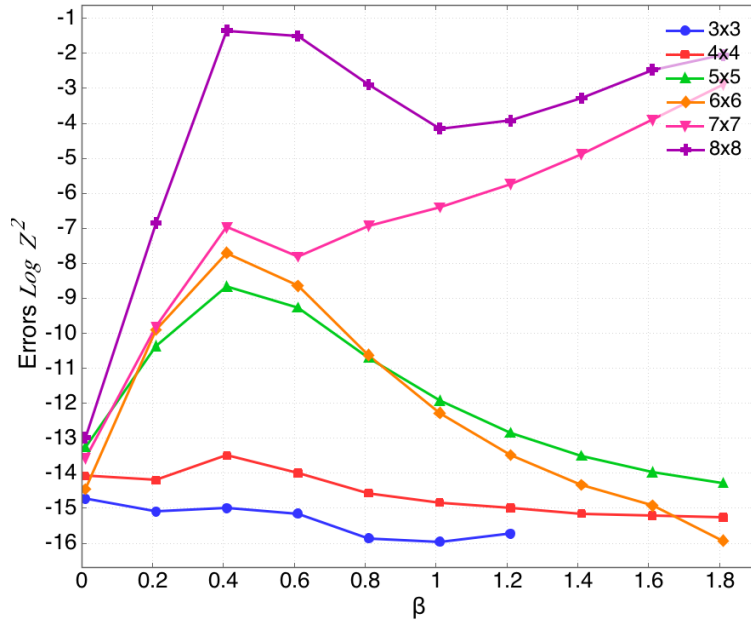


Figure 7: Logarithm of the relative errors in the reconstruction and analytic continuation of the square of the partition function of the classical ferromagnetic Ising model with open boundary conditions as a function of the inverse temperature. Each curve is the relative error for a different system size. For all system sizes the error shows a peak near the critical point. However, for systems larger than 7×7 the error grows quickly as the temperature approaches zero.

plot presented here, an upper bound on the ground state energy is then obtained by looking at the point where the two curves intersect. As one can see, the result for this instance is very good, but, generically speaking, the impossibility to rule out worst cases scenarios, does not allow us to give more quantitative results.

In the same way that protocol 2 can be used to estimate the real temperature partition function via measurements of the quantum overlap $\langle \Phi | \Psi \rangle$ and an analytic continuation, protocol 1 can be used to estimate the square of the real temperature partition function via measurements of the square of the overlap $|\langle \Phi | \Psi \rangle|^2$. The only difference is that as the function to reconstruct is squared, the frequencies of the modes in the Fourier series that we construct from experimental data is doubled. Hence, for protocol 1 more measurements are needed, double the amount needed in protocol 2. We have reconstructed the square of the partition function of a classical Ising model in 2D and performed the analytic continuation. For a study of the errors in the reconstruction see Fig.7.

B Proof of theorem 4.1

Let us start with the following classical result [22]

Theorem B.1 (Berry-Esséen) *Let $W_1 \dots W_L$ denote L independent random variables such that $\langle W_k \rangle = 0, 0 < \langle W_k^2 \rangle < \infty, \langle |W_k|^3 \rangle < \infty, k \in \{1 \dots L\}$. The cumulative distribution function \mathcal{F}_W of*

$$W \equiv \frac{W_1 + \dots + W_L}{(\sigma_1^2 + \dots + \sigma_L^2)^{1/2}}$$

satisfies the inequality

$$\|\mathcal{F}_W - \mathcal{F}_*\|_\infty \leq C_{BE} \sum_{k=1}^L \langle |W_k|^3 \rangle / \left(\sum_{k=1}^L \langle W_k^2 \rangle \right)^{3/2}, \quad (73)$$

where \mathcal{F}_ denotes the cumulative distribution of a zero-mean unit-variance Gaussian. The value of the constant C_{BE} is at most 0.56 [42].*

In the context of the estimation problem of Section 4, the r.h.s. of Eq.(73) reads

$$C_{BE} D_M \equiv C_{BE} \sum_j \frac{|\Re w^{(N)}(i\beta - \alpha_j)|^3 E_3(X_j)}{M^2} / \left(\sum_j \frac{|\Re w^{(N)}(i\beta - \alpha_j)|^2 E_2(X_j)}{M} \right)^{3/2}. \quad (74)$$

The quantities $E_2(X_j)$ and $E_3(X_j)$ are of course defined as in Section 4. Their values cannot be known exactly. But, from experimental data, one can construct estimates for them, $\hat{E}_2(X_j)$ and $\hat{E}_3(X_j)$ respectively, valid with high confidence. With such estimates, we can bound D_M as

$$D_M \leq D_M(\{\epsilon\}) = \frac{1}{M} \sum_j |\Re w^{(N)}(i\beta - \alpha_j)|^3 (\hat{E}_3(X_j) + \epsilon_j) / \left(\sum_j |\Re w^{(N)}(i\beta - \alpha_j)|^2 (\hat{E}_2(X_j) - \epsilon_j) \right)^{3/2}, \quad \epsilon_j > 0, \quad (75)$$

at a confidence level $\prod_j \text{Prob}[\{E_2(X_j) \geq \hat{E}_2(X_j) - \epsilon_j\} \cap \{E_3(X_j) \leq \hat{E}_3(X_j) + \epsilon_j\}]$. ($\{\epsilon\}$ is a shorthand notation for $\{\epsilon_j\}$). Let dA denote the random variable $\hat{A}_{RR}(i\beta) - A_{RR}(i\beta)$, and let \mathcal{F}_{dA} denote its cumulative.

By definition, $\text{Prob}[|dA| < \delta] = \mathcal{F}_{dA}(\delta) - \mathcal{F}_{dA}(-\delta)$. As just any cumulative distribution, \mathcal{F}_{dA} satisfies the scaling identity $\mathcal{F}_{dA}(y) = \mathcal{F}_{\lambda dA}(\lambda y)$, $\forall \lambda \geq 0$. Thus, with

$$\lambda_M = \sqrt{M / \sum_j |\Re w^{(N)}(i\beta - \alpha_j)|^2 \mathbb{E}_2(X_j)},$$

we can use the Berry-Esséen theorem to lower bound the probability of the event $\{|dA| < \delta\}$, *conditioned* on the event $\{D_M \leq D_M(\{\epsilon\})\}$:

$$\text{Prob}[\{|dA| < \delta\} | \{D_M \leq D_M(\{\epsilon\})\}] \geq 1 - 2\mathcal{F}_*(-\lambda_M \delta) - 2C_{BE} D_M(\{\epsilon\}).$$

Of course, cumulative functions are non-decreasing. Thus,

$$\text{Prob}[\{|dA| < \delta\} | \{[D_M \leq D_M(\{\epsilon\})] \cap [\lambda_M(\{\epsilon\}) \leq \lambda_M]\}] \geq 1 - 2\mathcal{F}_*(-\lambda_M(\{\epsilon\}) \delta) - 2C_{BE} D_M(\{\epsilon\})$$

where

$$\lambda_M(\{\epsilon\}) = \sqrt{M / \sum_j |\Re w^{(N)}(i\beta - \alpha_j)|^2 (\widehat{\mathbb{E}}_2(X_j) + \epsilon_j)}. \quad (76)$$

Finally, using Bayes' rule, we find that

$$\begin{aligned} \text{Prob}[|dA| < \delta] &= \text{Prob}[\{|dA| < \delta\} | \{[D_M \leq D_M(\{\epsilon\})] \cap [\lambda_M(\{\epsilon\}) \leq \lambda_M]\}] \times \\ &\quad \text{Prob}[\{D_M \leq D_M(\{\epsilon\})\} \cap \{\lambda_M(\{\epsilon\}) \leq \lambda_M\}] \\ &\geq \prod_j \text{Prob}[\{\widehat{\mathbb{E}}_2(X_j) + \epsilon_j \geq \mathbb{E}_2(X_j) \geq \widehat{\mathbb{E}}_2(X_j) - \epsilon_j\} \cap \{\mathbb{E}_3(X_j) \leq \widehat{\mathbb{E}}_3(X_j) + \epsilon_j\}] \times \\ &\quad [1 - 2\mathcal{F}_*(-\lambda_M(\{\epsilon\})\delta) - 2C_{BE} D_M(\{\epsilon\})], \quad \forall \delta, \{\epsilon\} > 0. \end{aligned} \quad (77)$$

We show in Appendix C that

$$\text{Prob}[\{\widehat{\mathbb{E}}_2(X_j) + \epsilon_j \geq \mathbb{E}_2(X_j) \geq \widehat{\mathbb{E}}_2(X_j) - \epsilon_j\} \cap \{\mathbb{E}_3(X_j) \leq \widehat{\mathbb{E}}_3(X_j) + \epsilon_j\}] \geq 1 - 2 \exp(-\epsilon_j M / 32), \quad \forall \epsilon_j > 0,$$

So, in particular, for fixed δ ,

$$\text{Prob}[|dA| < \delta] \geq \sup_{\{\epsilon\}} \prod_j (1 - 2 \exp(-\epsilon_j M / 32)) [1 - 2\mathcal{F}_*(-\lambda_M(\{\epsilon\})\delta) - 1.12 D_M(\{\epsilon\})], \quad (78)$$

from which Eq.(33) follows.

C Confidence intervals for moments of a binomial

Consider a binary random variable V characterised by some probability p for one of the values. Let \hat{p} denote our estimate for p , found after M Bernoulli trials. Let $\mathbb{E}_2(p)$ denote the variance of V . Clearly,

$$|\hat{p} - p| \leq \epsilon_0 \Rightarrow \mathbb{E}_2(p) \in [\mathbb{E}_2^-(\hat{p}, \epsilon_0), \mathbb{E}_2^+(\hat{p}, \epsilon_0)], \quad (79)$$

where $\mathbb{E}_2^-(\hat{p}, \epsilon_0) = \min\{\mathbb{E}_2(q) : |q - \hat{p}| < \epsilon_0\}$ and $\mathbb{E}_2^+(\hat{p}, \epsilon_0) = \max\{\mathbb{E}_2(q) : |q - \hat{p}| < \epsilon_0\}$. Similarly, if we denote $\mathbb{E}_3(p) = \langle |V|^3 \rangle$, we have that

$$|\hat{p} - p| \leq \epsilon_0 \Rightarrow \mathbb{E}_3(p) \in [\mathbb{E}_3^-(\hat{p}, \epsilon_0), \mathbb{E}_3^+(\hat{p}, \epsilon_0)], \quad (80)$$

where $E_3^-(\hat{p}, \epsilon_0) = \min\{E_3(q) : |q - \hat{p}| < \epsilon_0\}$ and $E_3^+(\hat{p}, \epsilon_0) = \max\{E_3(q) : |q - \hat{p}| < \epsilon_0\}$. For bookkeeping, let us attribute names to the various events we need to consider:

$$A \equiv \{|\hat{p} - p| \leq \epsilon_0\}, \quad B \equiv \{E_2(p) \in [E_2^-(\hat{p}, \epsilon_0), E_2^+(\hat{p}, \epsilon_0)]\}, \quad C \equiv \{E_3(p) \in [E_3^-(\hat{p}, \epsilon_0), E_3^+(\hat{p}, \epsilon_0)]\}.$$

Clearly, $A \subset B$ and $A \subset C$, so that $A \subset B \cap C$, and

$$\text{Prob}[B \cap C] \geq \text{Prob}[A] \geq 1 - 2 \exp(-\epsilon_0 M/4).$$

The last inequality is a consequence of Hoeffding's [22]. Next we define our estimate for the variance and the third moment as

$$s^2 = \frac{E_2^-(\hat{p}, \epsilon_0) + E_2^+(\hat{p}, \epsilon_0)}{2}, \quad r = \frac{E_3^-(\hat{p}, \epsilon_0) + E_3^+(\hat{p}, \epsilon_0)}{2}.$$

We also define $2\epsilon_1 = E_2^+(\hat{p}, \epsilon_0) - E_2^-(\hat{p}, \epsilon_0)$ and $2\epsilon_2 = E_3^+(\hat{p}, \epsilon_0) - E_3^-(\hat{p}, \epsilon_0)$. For any ϵ greater or equal to $\max\{\epsilon_1, \epsilon_2\}$, we have $B \subset B'$ and $C \subset C'$, where the events B' and C' are defined as

$$B' \equiv E_2(p) \in [s^2 - \epsilon, s^2 + \epsilon], \quad C' \equiv E_3(p) \in [r - \epsilon, r + \epsilon].$$

So, $\text{Prob}[B' \cap C'] \geq \text{Prob}[B \cap C] \geq 1 - 2 \exp(-\epsilon_0 M/4)$. Picking

$$\epsilon = \max\left\{\sup_{0 \leq q \leq 1} \frac{dE_2(p)}{dp} \Big|_q, \sup_{0 \leq q \leq 1} \frac{dE_3(p)}{dp} \Big|_q\right\} \times \epsilon_0 = 8 \epsilon_0,$$

we find that

$$\text{Prob}[\{s^2 - \epsilon \leq E_2(p) \leq s^2 + \epsilon\} \cap \{E_3 \leq r + \epsilon\}] \geq$$

$$\text{Prob}[\{s^2 - \epsilon \leq E_2(p) \leq s^2 + \epsilon\} \cap \{r - \epsilon \leq E_3 \leq r + \epsilon\}] \geq 1 - 2 \exp(-\epsilon M/32). \quad (81)$$

D Proof of Lemma 6.2

We begin with the discrete gate set

$$\mathfrak{G}_0 = \{Z_k(\pi/4), \text{Had}_k, k = 1 \dots n\} \cup \{\text{CNOT}_{k,k+1}, k = 1 \dots n-1\} \quad (82)$$

acting on an n qubit register that is universal for quantum computation [43]. By the Solovay-Kitaev [44] theorem an arbitrary polynomial sized quantum circuit can be efficiently approximate from this gate set with a polynomial overhead. To realize this using global operations in the mirror encoding of Raussendorf, one makes frequent use of the global shift operator $G_{\text{tot}} = \sigma_{\text{tot}}^z(\pi) \sigma_{\text{tot}}^y(\pi/2) \text{CP}_{\text{tot}}$, with the property that G_{tot}^{2n+1} is a reflection of the state of the chain about its middle. An arbitrary Z rotation on logical qubit k can be physically implemented as [14]

$$Z_k^{\text{logi}}(\alpha) = e^{i \frac{\alpha}{2} (\sigma_k^z + \sigma_{n-k+1}^z)} = G_{\text{tot}}^{n+1-k} \sigma_{\text{tot}}^y(\pi) G \sigma_{\text{tot}}^y(\pi) G^{k-1} \sigma_{\text{tot}}^z(-\alpha/2) G_{\text{tot}}^{n+1-k} \sigma_{\text{tot}}^y(\pi) G \sigma_{\text{tot}}^y(\pi) G^{k-1} \sigma_{\text{tot}}^z(\alpha/2). \quad (83)$$

Similarly, an X rotation on logical qubit k is

$$X_k^{\text{logi}}(\alpha) = e^{i \frac{\alpha}{2} (\sigma_k^x + \sigma_{n-k+1}^x)} = G_{\text{tot}}^{n-k} \sigma_{\text{tot}}^y(\pi) G \sigma_{\text{tot}}^y(\pi) G^k \sigma_{\text{tot}}^z(-\pi/2) \sigma_{\text{tot}}^y(\alpha/2) \sigma_{\text{tot}}^z(\pi/2)$$

$$G_{\text{tot}}^{n-k} \sigma_{\text{tot}}^y(\pi) G \sigma_{\text{tot}}^y(\pi) G^k \sigma_{\text{tot}}^z(-\pi/2) \sigma_{\text{tot}}^y(-\alpha/2) \sigma_{\text{tot}}^z(\pi/2). \quad (84)$$

Finally, an entangling gate between logical qubits k and $k + 1$ can be implemented as

$$V_{k,k+1}^{\text{logi}}(\alpha) = e^{i\alpha(\sigma_k^z \otimes \sigma_{k+1}^x + \sigma_{k+n}^z \otimes \sigma_{k+n-1}^x)} = G^k X_k^{\text{logi}}(\alpha) G^{\dagger k}. \quad (85)$$

Since $V_{k,k+1}(\pi/4)\text{Had}_{k+1}Z_k(\pi/2)Z_{k+1}(\pi/2)\text{Had}_{k+1} = \text{CNOT}_{k,k+1}$ then the gate set

$$\mathfrak{G}_1 = \{Z_k^{\text{logi}}(\pi/4), \text{Had}_k^{\text{logi}}, k = 1 \dots n\} \cup \{V_{k,k+1}(\pi/4), k = 1 \dots n-1\} \quad (86)$$

is universal for quantum computation. Now the Hadamard gate can be related to X and Z rotations through the identity $\text{Had} = \sigma^z(\pi/2)\sigma^x(\pi/2)\sigma^z(\pi/2)$. Also we note the following relations: $[\sigma^z(\pi/8)]^{31} = \sigma^z(-\pi/8)$, and $\sigma^y(\pm\pi/4) = \sigma^x(-\pi/2)\sigma^z(\mp\pi/4)\sigma^x(\pi/2)$ and also $\sigma^x(\pm\pi/2) = \sigma^z(\pm\pi/2)\text{Had}\sigma^z(\pm\pi/2)$. Then from Eqs.(83,84,85), we see that it is enough to be able to implement

$$\mathfrak{G} = \{\text{CP}_{\text{tot}}, \sigma_{\text{tot}}^z(\pi/8), \text{Had}_{\text{tot}}\}$$

in order to achieve universal quantum computation.

E Magnetisation and Approximation Schemes

The first part of our construction closely follows a general argument presented in Ref. [26], and establishes a connection between partition function evaluations and the ability to draw samples from Boltzmann probability distributions. Some adaptations were made, though. We felt that indicating only these adaptations would have resulted in an awkward presentation. This is why, for the sake of clarity, we have chosen to reproduce this argument, with these adaptations included, in a concise but self-contained manner. In the second part of our construction, we show how measurements of magnetisation on specific non-homogeneous Ising models allow to draw from Boltzmann distributions. Consider thus the Ising model on a two-dimensional square lattice Λ , described by the Hamiltonian:

$$H(\sigma) = -J \sum_{\langle i,j \rangle} \sigma_i \sigma_j - h \sum_{i \in \Lambda} \sigma_i. \quad (87)$$

For $h = 0$, the model is solvable and $Z(h = 0)$ is known exactly (see e.g. [23]). We wish to evaluate the partition function at a fixed temperature⁴ β , $Z(h)$, for $h > 0$, say⁵. For that purpose, we express $Z(h)$ as

$$Z(h) = \frac{Z(h_L)}{Z(h_{L-1})} \times \frac{Z(h_{L-1})}{Z(h_{L-2})} \times \dots \times \frac{Z(h_1)}{Z(h_0)} \times Z(h_0), \quad (88)$$

where $0 = h_0 < h_1 < \dots < h_L = h$. These values h_k are chosen to be equally spaced, and we will denote the spacing $h_k - h_{k-1}$ by δh . Each ratio $\varrho_k = Z(h_k)/Z(h_{k-1})$ can be expressed as

$$\varrho_k = \sum_{\sigma} \frac{e^{-\beta H_{k-1}(\sigma)}}{Z(h_{k-1})} e^{\beta \delta h |\Lambda| M(\sigma)} \equiv \sum_{\sigma} \pi_{k-1}(\sigma) e^{\beta \delta h |\Lambda| M(\sigma)}, \quad (89)$$

where $M(\sigma)$ denotes the mean magnetisation of the system when the lattice is in configuration σ , $|\Lambda|$ denotes again the size of the lattice Λ , and where H_{k-1} is a shorthand notation for the hamiltonian when the magnetic field is set to h_{k-1} .

⁴Change of notations: Since we will work at constant temperature, we will from now drop β and simply write $Z(h)$ instead of $Z(\beta, h)$.

⁵The case $h < 0$ is treated similarly.

In order to evaluate $Z(h)$, we will use a collection of estimators for the quantities ϱ_k , each involving n sample configurations. These estimators are defined as

$$\hat{\varrho}_k : \{\sigma_k^{(1)}, \dots, \sigma_k^{(n)}\} \rightarrow \hat{\varrho}_k(\sigma_k^{(1)}, \dots, \sigma_k^{(n)}) = \frac{1}{n} \sum_{j=1}^n e^{\beta|\Lambda|\delta h M(\sigma_k^{(j)})}, \quad (90)$$

where each sample $\sigma_k^{(j)}$ is drawn according to some probability distribution π'_{k-1} . Our estimator for $Z(h)$ is

$$\hat{Z}(h) \equiv \prod_{k=1}^L \hat{\varrho}_k Z(h_0).$$

Let $\bar{\varrho}_k$ denote the mean value of $\hat{\varrho}_k$, i.e.

$$\bar{\varrho}_k = \sum_{\sigma_k^{(1)}} \dots \sum_{\sigma_k^{(n)}} \pi'_{k-1}(\sigma_k^{(1)}) \dots \pi'_{k-1}(\sigma_k^{(n)}) \hat{\varrho}_k(\sigma_k^{(1)}, \dots, \sigma_k^{(n)}).$$

Since all $\hat{\varrho}_k$ are independent random variables, we find that the mean value of $\hat{Z}(h)$ is given by $\bar{Z}(h) = \prod_{k=1}^L \bar{\varrho}_k Z(h_0)$. Now let us assume that

$$|Z(h) - \bar{Z}(h)| \leq \epsilon' Z(h), \quad (91)$$

and that

$$|\bar{Z}(h) - \hat{Z}(h)| \leq \delta \bar{Z}(h), \quad (92)$$

with probability at least, $3/4$ say ⁶. Then

$$(1 - \delta)(1 - \epsilon')Z(h) \leq \hat{Z}(h) \leq (1 + \delta)(1 + \epsilon')Z(h),$$

with probability at least $3/4$. Thus

$$(1 - \epsilon)Z(h) \leq \hat{Z}(h) \leq (1 + \epsilon)Z(h) \quad (93)$$

with probability at least $3/4$ whenever $\epsilon \geq \delta + \epsilon' + \delta\epsilon'$.

Clearly,

$$e^{-\beta\delta h|\Lambda|} \leq e^{\beta|\Lambda|\delta h M(\sigma)} \leq e^{\beta\delta h|\Lambda|} \quad \forall \sigma.$$

Plugging these inequalities into Hoeffding's inequality [22], we find that

$$\text{Prob}[|\hat{\varrho}_k - \bar{\varrho}_k| \leq \zeta] \geq 1 - 2e^{-2n\zeta^2 / \sinh(|\Lambda|\beta\delta h)^2}. \quad (94)$$

Let us use this latter relation in order to construct an upper bound on $|\hat{Z}(h) - \bar{Z}(h)|$ valid with tunable probability. We will use the following Lemma:

Lemma E.1

$$|\hat{Z}(h) - \bar{Z}(h)| \leq \left| \prod_{k=1}^L \left(1 + \frac{\zeta}{\bar{\varrho}_k}\right) - 1 \right| \bar{Z}(h) \quad (95)$$

with probability at least $(1 - 2e^{-2n\zeta^2 / \sinh(|\Lambda|\beta\delta h)^2})^L$.

⁶This value is somewhat arbitrary. As explained in Ref.[26], any level of confidence strictly above $1/2$ can be efficiently boosted to arbitrarily close to 1.

Proof: We start with the following identity

$$|\hat{Z}(h) - \bar{Z}(h)| = \left| \prod_{k=1}^L \hat{\varrho}_k - \prod_{k=1}^L \bar{\varrho}_k \right| Z(h_0) = \left| \prod_{k=1}^L \left(1 + \frac{\hat{\varrho}_k - \bar{\varrho}_k}{\bar{\varrho}_k}\right) - 1 \right| \bar{Z}(h)$$

Next, we have the inequality

$$\left| \prod_{k=1}^L (1 + x_k) - 1 \right| \leq \left| \prod_{k=1}^L (1 + |x_k|) - 1 \right|, \quad \forall x_k \in \mathbb{R}. \quad (96)$$

Let us consider two cases: (i) $\prod_{k=1}^L (1 + x_k) - 1 \geq 0$, (ii) $\prod_{k=1}^L (1 + x_k) - 1 < 0$. The inequality is trivial in case (i). In case (ii), we need to prove that

$$1 - \prod_{k=1}^L (1 + x_k) \leq \prod_{k=1}^L (1 + |x_k|) - 1,$$

or $2 \leq \prod_{k=1}^L (1 + |x_k|) + \prod_{k=1}^L (1 + x_k)$. The r.h.s. of this last inequality can certainly be written as

$$2 + \sum_{i_1} \dots \sum_{i_L} \varkappa_{i_1 \dots i_L} (|x_1|^{i_1} \dots |x_L|^{i_L} + x_1^{i_1} \dots x_L^{i_L}),$$

where each coefficient $\varkappa_{i_1 \dots i_L}$ is non-negative. It is also clear that each quantity $(|x_1|^{i_1} \dots |x_L|^{i_L} + x_1^{i_1} \dots x_L^{i_L})$ is non-negative. Inequality (96) implies that

$$|\hat{Z}(h) - \bar{Z}(h)| \leq \left| \prod_{k=1}^L \left(1 + \frac{|\hat{\varrho}_k - \bar{\varrho}_k|}{\bar{\varrho}_k}\right) - 1 \right| \bar{Z}(h).$$

The r.h.s of this relation is lower than $\left| \prod_{k=1}^L \left(1 + \frac{\zeta}{\bar{\varrho}_k}\right) - 1 \right| \bar{Z}(h)$ with probability at least $(1 - 2e^{-2n\zeta^2 / \sinh(|\Lambda|\beta\delta h)^2})^L$ (Hoeffding's inequality). \square

We will pick the spacing between two consecutive magnetisations to be $\delta h = \frac{\eta}{\beta|\Lambda|}$, where η is some positive constant we are free to choose at our convenience. δh fixes the value of L to

$$L = (h - h_0)\beta|\Lambda|/\eta. \quad (97)$$

With a given choice for δh , we have that $\bar{\varrho}_k \geq e^{-\eta}$ and

$$|\hat{Z}(h) - \bar{Z}(h)| \leq |(1 + e^{\eta\zeta})^L - 1| \bar{Z}(h), \quad (98)$$

with probability at least $(1 - 2e^{-2n\zeta^2 / \sinh(|\Lambda|\beta\delta h)^2})^L$. How should we pick ζ in order to ensure that the l.h.s. of (98) is smaller than $\delta \bar{Z}(h)$ for some fixed δ ? Since $(1 + e^{\eta\zeta})^L \leq e^{L\zeta e^\eta}$, it is enough that

$$\zeta \leq \frac{\ln(1 + \delta)}{Le^\eta}.$$

We also wish to know how, for fixed values of ζ, L, η , we should choose n in order to guarantee a level of confidence at least equal to $3/4$. Direct substitution shows that the condition

$$(1 - 2e^{-2n\zeta^2 / \sinh(\eta)^2})^L \geq 3/4$$

is satisfied if

$$n \geq -\frac{\sinh \eta^2 e^{2\eta} L^2}{2(\ln(1+\delta))^2} \ln \left[\frac{1}{2} \left(1 - \left(\frac{3}{4} \right)^{1/L} \right) \right]. \quad (99)$$

To summarise, for L satisfying (97) and n satisfying (99), the partition function estimator satisfies

$$\text{Prob}[|\hat{Z}(h) - \bar{Z}(h)| \leq \delta \bar{Z}(h)] \geq 3/4. \quad (100)$$

Next we wish to establish a condition that guarantees that Inequality (91) holds. We start by observing that

$$|\bar{Z}(h) - Z(h)| \leq \left| \prod_{k=1}^L \left(1 + \frac{|\varrho_k - \bar{\varrho}_k|}{\varrho_k} \right) - 1 \right| Z(h).$$

Let

$$\Delta\pi_{k-1} \equiv \max_S |\pi_{k-1}(S) - \pi'_{k-1}(S)| = \frac{1}{2} \sum_{\sigma} |\pi_{k-1}(\sigma) - \pi'_{k-1}(\sigma)|$$

denote the total variation⁷ between the probability distributions π_{k-1} and π'_{k-1} . Let us also denote $\Delta\pi^* = \max_k \Delta\pi_{k-1}$. We see that

$$|\varrho_k - \bar{\varrho}_k| \leq e^\eta \Delta\pi^*, \quad \rho_k \geq e^{-\eta} \quad \forall k.$$

Thus

$$|Z(h) - \bar{Z}(h)| \leq [(1 + e^{2\eta} \Delta\pi^*)^L - 1] Z(h) \leq (e^{Le^{2\eta} \Delta\pi^*} - 1) Z(h). \quad (101)$$

So it is enough that

$$\Delta\pi^* \leq \frac{e^{-2\eta}}{L} \ln(1 + \epsilon').$$

On another hand, $\Delta\pi_{k-1}$ satisfies the inequality

$$\Delta\pi_{k-1} \leq \frac{1}{2} \max_{\sigma} \left| 1 - \frac{\pi'_{k-1}(\sigma)}{\pi_{k-1}(\sigma)} \right|.$$

Using Bayes' theorem, to express π_{k-1} in terms of marginal and conditional probability distributions,

$$\pi_{k-1}(\sigma_1 \dots \sigma_{|\Lambda|}) = \pi_{k-1}^{(1)}(\sigma_1) \pi_{k-1}^{(2)}(\sigma_2 | \sigma_1) \dots \pi_{k-1}^{(|\Lambda|)}(\sigma_{|\Lambda|} | \sigma_1 \dots \sigma_{|\Lambda|-1}), \quad (102)$$

the r.h.s of the latter inequality can be written as

$$\frac{1}{2} \max_{\sigma} \left| \prod_{l=1}^{|\Lambda|} \frac{\pi_{k-1}'^{(l)}(\sigma_l | \sigma_1 \dots \sigma_{l-1})}{\pi_{k-1}^{(l)}(\sigma_l | \sigma_1 \dots \sigma_{l-1})} - 1 \right|.$$

If we use the *finesse*

$$\mathfrak{f} \equiv \max_{k,l,\sigma} \frac{|\pi_{k-1}'^{(l)}(\sigma_l | \sigma_1 \dots \sigma_{l-1}) - \pi_{k-1}^{(l)}(\sigma_l | \sigma_1 \dots \sigma_{l-1})|}{\pi_{k-1}^{(l)}(\sigma_l | \sigma_1 \dots \sigma_{l-1})} \quad (103)$$

to quantify the accuracy with which the distributions $\{\pi_{k-1}'\}$ approach the distributions $\{\pi_{k-1}\}$, we see that $\Delta\pi^* \leq \frac{1}{2} |(1 + \mathfrak{f})^{|\Lambda|} - 1| \leq \frac{1}{2} (e^{\mathfrak{f}|\Lambda|} - 1)$. So $|Z(h) - \bar{Z}(h)| \leq \epsilon' Z(h)$ whenever the finesse satisfies

$$\mathfrak{f} \leq \frac{1}{|\Lambda|} \ln \left[1 + \frac{2e^{-2\eta}}{|\Lambda|} \ln(1 + \epsilon') \right]. \quad (104)$$

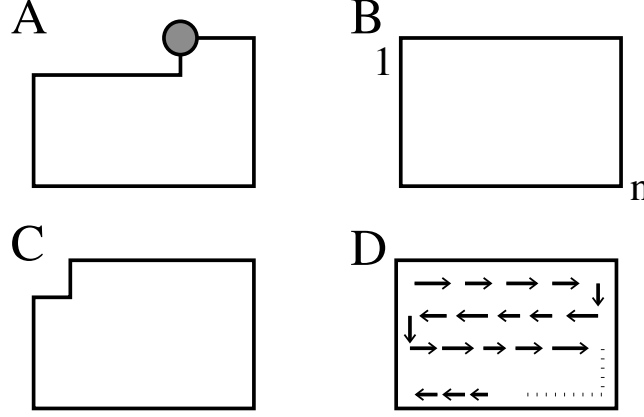


Figure 8: A. Typical corner on which magnetisations need to be measured in order to get an approximation for the partition function of the Ising model defined on a square lattice. B. Labelling of spins of the original lattice. C. Lattice obtained after the spin on one corner has been fixed. D. Cartoon for a possible choice to run over all spins of the original lattice

We now turn to the second part of our construction and explain how it is possible to get samples for the estimators \hat{q}_k from corner single site magnetisation estimates, as indicated on Fig.8-A. Assume that the $|\Lambda|$ particles of the lattice are numbered as indicated on Fig.8-B. For fixed external field h_{k-1} , It is clear that the magnetisation on the corner '1' is given by

$$m_{k-1}(1) = \frac{1}{Z(h_{k-1})} \sum_{\sigma} e^{-\beta H_{k-1}(\sigma)} \sigma_1 = \pi_{k-1}^{(1)}(\uparrow) - \pi_{k-1}^{(1)}(\downarrow).$$

From an estimate $m'_{k-1}(1)$, we construct $\pi'^{(1)}_{k-1}(\sigma_1)$ as

$$\pi'^{(1)}_{k-1}(\uparrow) = \frac{1 + m'_{k-1}(1)}{2}, \quad \pi'^{(1)}_{k-1}(\downarrow) = \frac{1 - m'_{k-1}(1)}{2}. \quad (105)$$

It is certainly possible to draw *exactly* according to this distribution $\pi'^{(1)}_{k-1}$; it is a *known* two-outcome probability distribution. Let us imagine we do it and obtain an outcome x_1 . Then we consider another Ising system, identical to the original apart from the fact that the spin labelled '1' is now fixed to x_1 . This new system is now defined on the geometry indicated by Fig.8-C ($|\Lambda| - 1$ spins), and governed by the Ising Hamiltonian:

$$H^{(2)}(\sigma_2 \dots \sigma_{|\Lambda|}) = H_{k-1}(x_1 \sigma_2 \dots \sigma_{|\Lambda|}),$$

and its Boltzmann weights obey

$$\frac{e^{-\beta H^{(2)}(\sigma_2 \dots \sigma_n)}}{Z^{(2)}} = \pi_{k-1}^{(2)}(\sigma_2 | x_1) \dots \pi_{k-1}^{(|\Lambda|)}(\sigma_{|\Lambda|} | x_1 \dots \sigma_{|\Lambda|-1}).$$

If we now measure the magnetisation at corner '2' for this new system, we get

$$m'_{k-1}(2|x_1) \simeq m_{k-1}(2|x_1) = \pi_{k-1}^{(2)}(\uparrow | x_1) - \pi_{k-1}^{(2)}(\downarrow | x_1)$$

⁷To obtain the last equality, one observes that if an event S_* achieves the maximum, so does the complementary event S_*^c .

The magnetisation $m'_{k-1}(2|x_1)$ allows to construct

$$\pi'_{k-1}(\uparrow|x_1) = \frac{1 + m'_{k-1}(2|x_1)}{2}, \quad \pi'_{k-1}(\downarrow|x_1) = \frac{1 - m'_{k-1}(2|x_1)}{2}. \quad (106)$$

Again, this known probability distribution is simple enough that it is possible to draw exactly a sample x_2 according to it. Repeating this reasoning, running along the lattice in the order indicated by the cartoon on Fig.8-D, we see that the ability to estimate corner magnetisations combined with Bayes' theorem allows to draw sequentially⁸ according to

$$\pi'_{k-1}(\sigma_1 \dots \sigma_{|\Lambda|}) = \pi'^{(1)}_{k-1}(\sigma_1) \pi'^{(2)}_{k-1}(\sigma_2|\sigma_1) \dots \pi'^{(|\Lambda|)}_{k-1}(\sigma_{|\Lambda|}|\sigma_1 \dots \sigma_{|\Lambda|-1}).$$

Finally, we observe that

$$\frac{|\pi'^{(l)}_{k-1}(\sigma_l|\sigma_1 \dots \sigma_{l-1}) - \pi^{(l)}_{k-1}(\sigma_l|\sigma_1 \dots \sigma_{l-1})|}{\pi^{(l)}_{k-1}(\sigma_l|\sigma_1 \dots \sigma_{l-1})} \leq \frac{|m'_{k-1}(l|\sigma_1 \dots \sigma_{l-1}) - m_{k-1}(l|\sigma_1 \dots \sigma_{l-1})|}{|1 - |m_{k-1}(l|\sigma_1 \dots \sigma_{l-1})||}.$$

So the condition (104) leads simply to a condition on the *relative* precision over the magnetisation.

Summarising, *for any $\epsilon > 0$, temperature β and magnetic field h , it is possible to provide an estimate $\hat{Z}(h)$ for the ferromagnetic Ising partition function $Z(h)$ satisfying*

$$\text{Prob}[|\hat{Z}(h) - Z(h)| \leq \epsilon Z(h)] \geq 3/4, \quad (107)$$

in a time that scales at most polynomially with $\beta, \epsilon^{-1}, |h|$, and the size of the system if we are able to perform corner magnetisation measurements on related non-homogeneous Ising systems. The required relative precision need not be lower than the inverse of some polynomial in $|h|, \beta, \epsilon^{-1}$ and the size of the system.

F Proof of Theorem 6.3

Our starting point is the following direct consequence of the adiabatic theorem, as stated in [29].

Lemma F.1 *Let $\gamma = \min_{t \in [0:T]} \text{gap } \hat{H}(t)$, where $\text{gap } \hat{H}(t)$ denotes the difference between the two lowest eigenvalues of $\hat{H}(t)$, and let $|\Phi'\rangle$ denote the quantum state obtained by the continuous evolution induced on $|\Phi_0\rangle$ by the Hamiltonian family (47). Let also $|\Lambda|$ and $|E(\Lambda)|$ denote respectively the number of sites and edges of the lattice Λ . The distance between $|\Phi'\rangle$ and the true ground state $|G\rangle$ is at most δ whenever T satisfies*

$$T \geq T_*(\hat{H}, \delta) = \frac{10^5}{\delta^2} \frac{(|h| \cdot |\Lambda| + |J| \cdot |E(\Lambda)|)^3}{\gamma^4}. \quad (108)$$

Proof: Let us introduce the parameter $s = t/T$. Theorem 2.1 of Ref.[29] provides the following sufficient condition for adiabaticity⁹:

$$T \geq T_*(\hat{H}, \delta) = \frac{10^5}{\delta^2} \max_{0 \leq s \leq 1} \max \left\{ \left\| \frac{d}{ds} \hat{H} \right\|_\infty^3, \frac{\left\| \frac{d}{ds} \hat{H} \right\|_\infty \cdot \left\| \frac{d^2}{ds^2} \hat{H} \right\|_\infty}{\gamma^3} \right\} \quad (109)$$

⁸The order we have chosen has no particular meaning. The reasoning is of course valid for any labelling of the sites of the lattices.

⁹In the following $\|A\|_\infty$ will denote the operator norm of an operator A , i.e. $\|A\|_\infty = \sup_x \frac{\|Ax\|_2}{\|x\|_2}$.

valid for any time-dependent hamiltonian $\hat{H}(t)$. Adapting this condition to the special case of Hamiltonians (47), we see the r.h.s of (108) certainly upper bounds the r.h.s of (109). \square

We wish to discretise the time evolution of our system. Instead of considering the time-dependent evolution associated with the Hamiltonians $\hat{H}(t)$, we will deal with L consecutive *constant* unitary operators, $\mathcal{U}_k = \text{Exp}(-i\tau \hat{H}_0 - i\tau \hat{H}_1(k\tau))$, $k = 0 \dots L-1$, where we define the discretisation step as

$$\tau \equiv T/L. \quad (110)$$

We wish to work with the state $|\Phi^*\rangle = \mathcal{U}_{L-1} \dots \mathcal{U}_0 |+\rangle_x^{\otimes |\Lambda|}$ rather than with the state $|\Phi'\rangle$. Of course when L grows large we expect this substitution to have negligible effect. But we need to be precise and quantify the induced error. The following lemma addresses this issue.

Lemma F.2 *The distance between $|G\rangle$ and $|\Phi^*\rangle$ is bounded as*

$$||\Phi^*\rangle - |G\rangle|| \leq \delta + T \sqrt{\frac{2(|h| \cdot |\Lambda| + |J| \cdot |E(\Lambda)|)}{L}}, \quad (111)$$

whenever $T \geq T_*(\hat{H}, \delta)$.

Proof: The triangular inequality yields

$$||\Phi^*\rangle - |G\rangle|| \leq ||\Phi'\rangle - |G\rangle|| + ||\Phi^*\rangle - |\Phi'\rangle||. \quad (112)$$

The first term of the r.h.s of this expression is of course bounded by δ . To bound the second, we use Lemma 1 of [45], which states that if two time-dependent Hamiltonians $H_a(t), H_b(t), 0 \leq t \leq T$ differ at most by ϵ in operator norm for every t , then the difference between the unitary evolutions they induce, $\mathcal{U}_a(T), \mathcal{U}_b(T)$ satisfy $||\mathcal{U}_a(T) - \mathcal{U}_b(T)||_\infty \leq \sqrt{2T}\epsilon$. For every $t \in [0, T]$, let $k(t) \in \{0, \dots, L-1\}$ such that $k(t)\tau \leq t \leq (k(t)+1)\tau$. Clearly, $||\hat{H}(t) - \hat{H}(k(t)\tau)|| \leq \tau(|h| \cdot |\Lambda| + |J| \cdot |E(\Lambda)|)$. Identifying the r.h.s. of this inequality with ϵ and bearing in mind the definition of τ , one bounds the second term of the r.h.s. of (112) in the desired way. \square

Next, we split each unitary \mathcal{U}_k into a part that depends only on \hat{H}_0 and a part that depends only on $\hat{H}_1(k\tau)$: for τ small enough, each unitary \mathcal{U}_k can be safely replaced by the operator

$$U_k = e^{-i\tau \hat{H}_0} e^{-i\tau \hat{H}_1(k\tau)}. \quad (113)$$

Indeed, the Baker-Campbell-Hausdorff identity [45] implies that

$$||\mathcal{U}_k - U_k||_\infty \leq K(|h| \cdot |\Lambda| + |J| \cdot |E(\Lambda)|) \cdot (|h_\perp| \cdot |\Lambda|)\tau^2, \quad (114)$$

for some *constant* K . Then we arrive at the following:

Lemma F.3 *The quantity by which the state $U_{L-1}U_{L-2} \dots U_0 |+\rangle_x^{\otimes |\Lambda|}$ deviates from the true ground state of H^* is at most*

$$\Delta = \delta + T \sqrt{\frac{2(|h| \cdot |\Lambda| + |J_\parallel| \cdot |E(\Lambda)|)}{L}} + KL(|h| \times |\Lambda| + |J_\parallel| \times |E(\Lambda)|) \times |h_\perp| \cdot |\Lambda| \tau^2. \quad (115)$$

Proof: The result follows by combining the inequality in Eq. 114 with the Lemmata F.1, F.2. \square

G Approximation of fidelity overlaps

In this section we describe how to reconstruct fidelity overlap which is proportional to a partition function with complex couplings by sampling from partition functions with real couplings. We begin by rewriting Eq. 60 using more compact notation:

$$Z(\vec{\beta}) = B(\vec{\beta}) \sum_{g_1=-n_1}^0 \sum_{g_2=-n_2}^0 \sum_{g_3=-n_3}^0 \sum_{g_4=-n_4}^0 \sum_{g_5=-n_5}^0 \sum_{g_6=-n_6}^0 \tilde{c}_{g_1, g_2, g_3, g_4, g_5, g_6} e^{\sum_{j=1}^6 \beta^j g_j}, \quad (116)$$

where $\vec{\beta} = \{\beta^1, \beta^2, \beta^3, \beta^4, \beta^5, \beta^6\} \equiv \{\beta_+, \beta_-, \beta'_+, \beta'_-, \beta, \beta'\}$,

$$n_1 = n_2 = 2L|\Lambda|, \quad n_3 = n_4 = 2L'|\Lambda|, \quad n_5 = L(L-1)(|\Lambda|-1), \quad n_6 = L'(L'-1)(|\Lambda|-1).$$

and where $B(\vec{\beta}) = \prod_{j=1}^6 B_j(\beta^j)$ with $B_j(\beta^j) = e^{\frac{1}{2}n_j\beta^j}$ and \tilde{c} is just a relabeling of c with each index g_j ranging from $[0, n_j]$ rather than $[-n_j/2, n_j/2]$.

Let us define the polynomial:

$$p(\vec{x}) = p(x_1, x_2, x_3, x_4, x_5, x_6) = \sum_{i_1=0}^{n_1} \sum_{i_2=0}^{n_2} \sum_{i_3=0}^{n_3} \sum_{i_4=0}^{n_4} \sum_{i_5=0}^{n_5} \sum_{i_6=0}^{n_6} \tilde{c}_{i_1, i_2, i_3, i_4, i_5, i_6} x_1^{i_1} x_2^{i_2} x_3^{i_3} x_4^{i_4} x_5^{i_5} x_6^{i_6}, \quad (117)$$

where $\vec{x} = \{x_1, x_2, x_3, x_4, x_5, x_6\} \in \mathbb{R}^6$. Introducing the notation:

$$x_j(\cdot) = e^{-(\cdot)},$$

one has the trivial relation:

$$p(x_1(\beta_+), x_2(\beta_-), x_3(\beta'_+), x_4(\beta'_-), x_5(\beta), x_6(\beta')) = B^{-1}(\vec{\beta})Z(\vec{\beta}). \quad (118)$$

Note that, for physical temperatures, the domain of the polynomial is such that $x_j > 0$ and $||x_j|| \leq 1$ for $j = 1, \dots, 6$. We now want to reconstruct the polynomial $p(\vec{x})$ from a set of N data values $p(\vec{x}_i)$ with $\vec{x}_i \in \Gamma$ where Γ is a certain lattice of points in \mathbb{R}^6 . Although several options are available, in our case the polynomial is such that the simplest possible option can be used: a rectangular mesh lattice as:

$$\Gamma = \{x_{1, i_1=1}, \dots, x_{1, i_1=n_1+1}\} \times \dots \times \{x_{6, i_6=1}, \dots, x_{6, i_6=n_6+1}\}.$$

This is justified by the fact that, as we constructed it, the polynomial $p(\vec{x})$ has degree at most n_j in x_j ($j = 1, \dots, 6$). This means that $p(\vec{x})$ actually lies in the product space $\Pi_{n_1} \times \dots \times \Pi_{n_6}$, where Π_n indicates the space of univariate polynomials of degree at most n . Explicitely, the data values are written as:

$$p(\vec{x}_i) \equiv p(x_{1, i_1}, x_{2, i_2}, x_{3, i_3}, x_{4, i_4}, x_{5, i_5}, x_{6, i_6}) \equiv p_{i_1 i_2 i_3 i_4 i_5 i_6}.$$

The reconstructed polynomial can then be written as:

$$p(\vec{x}) = \sum_i p_{i_1 i_2 i_3 i_4 i_5 i_6} l_{i_1 i_2 i_3 i_4 i_5 i_6}(\vec{x}), \quad (119)$$

where:

$$l_{i_1 i_2 i_3 i_4 i_5 i_6}(\vec{x}) = l_{1, i_1}(x_1) l_{2, i_2}(x_2) l_{3, i_3}(x_3) l_{4, i_4}(x_4) l_{5, i_5}(x_5) l_{6, i_6}(x_6),$$

with:

$$l_{j,i_j}(x) = \prod_{\substack{k_j=1 \\ k_j \neq i_j}}^{n_j+1} \frac{x - x_{j,k_j}}{x_{j,i_j} - x_{j,k_j}} . \quad (120)$$

We now suppose to have a device that provides an estimate $\widehat{Z}(\beta)$ for the partition function, $Z(\beta)$, that satisfies

$$|\widehat{Z}(\beta) - Z(\beta)| \leq \delta , \quad (121)$$

and, from this, we want to see how well we can estimate the previously defined overlaps. Since the overlaps depend on the analitically continued partition function $Z(\vec{\beta}^*)$, we are going to show how to reconstruct it. From Eq. 118 and Eq. 119 we can write:

$$\begin{aligned} Z(\vec{\beta}^*) &= B(\vec{\beta}^*) p(x_1(\beta_+^*), x_2(\beta_-^*), x_3(\beta_+^*), x_4(\beta_-^*), x_5(\beta^*), x_6(\beta'^*)) = \\ &= B(\vec{\beta}^*) \sum_i p_{i_1 i_2 i_3 i_4 i_5 i_6} \prod_{j=1}^6 l_{j,i_j}(\vec{x}^j(\vec{\beta}^{*j})) . \end{aligned} \quad (122)$$

Now the coefficients $p_{i_1 i_2 i_3 i_4 i_5 i_6}$ are the values of the polynomial evaluated at the lattice points \vec{x}_i , and we can use the real temperatures oracle for the partition function in order to write:

$$Z(\vec{\beta}^*) = B(\vec{\beta}^*) \sum_{\vec{i}} B^{-1}(\vec{\beta}_{\vec{i}}) Z(\vec{\beta}_{\vec{i}}) \prod_{j=1}^6 l_{j,i_j}(\vec{x}^j(\vec{\beta}^{*j})) , \quad (123)$$

where $\vec{\beta}_{\vec{i}}$ represents the lattice Γ transformed in “ β coordinates”:

$$\begin{aligned} \vec{\beta}_{\vec{i}} &\equiv \{ \beta_{+,i_1}, \beta_{-,i_2}, \beta'_{+,i_3}, \beta'_{-,i_4}, \beta_{i_5}, \beta'_{i_6} \} \equiv \\ &\equiv \{ -\log x_{1,i_1}, -\log x_{2,i_2}, -\log x_{3,i_3}, -\log x_{4,i_4}, -\log x_{5,i_5}, -\log x_{6,i_6} \}. \end{aligned} \quad (124)$$

We also want to make an explicit choice for this lattice:

$$\vec{x}_{i_j}^j \equiv \frac{i_j}{n_j + 1} \text{ with: } i_j = 1, \dots, n_j + 1 , \quad (125)$$

which clearly satisfies the properties of the rectangular mesh Γ we stated before. Explicitly the mapping of this lattice in the “temperature domain” reads:

$$\vec{\beta}_{i_j}^j = -\log \frac{i_j}{n_j + 1} . \quad (126)$$

Now, we can write the final formula for the overlap as a function of the estimation of the partition function at real temperatures as:

$$f = \frac{1}{2^{|\Lambda|}} \left[\sqrt{\frac{1 - \epsilon^2}{\epsilon^4 + 4}} \right]^{L|\Lambda|} \left[\sqrt{\frac{1 - \epsilon'^2}{\epsilon'^4 + 4}} \right]^{L'|\Lambda|} B(\vec{\beta}^*) \sum_{\vec{i}} B^{-1}(\vec{\beta}_{\vec{i}}) Z(\vec{\beta}_{\vec{i}}) \prod_{j=1}^6 l_{j,i_j}(\vec{x}^j(\vec{\beta}^{*j})) . \quad (127)$$

We are interested in studying how the variance on this quantity scales. We have:

$$\sigma_f^2 \leq \frac{1}{2^{2(L+L'+1)|\Lambda|}} |B(\vec{\beta}^*)|^2 \sum_{\vec{i}} |B^{-1}(\vec{\beta}_{\vec{i}})|^2 \sigma_{Z(\vec{\beta}_{\vec{i}})}^2 \prod_{j=1}^6 |l_{j,i_j}(\vec{x}^j(\vec{\beta}^{*j}))|^2 . \quad (128)$$

From Eq. 121 we have:

$$\sigma_f^2 \leq \frac{1}{2^{2(L+L'+1)|\Lambda|}} |B(\vec{\beta}^*)|^2 \sum_{\vec{i}} \delta_i^2 |B^{-1}(\vec{\beta}_{\vec{i}})|^2 \prod_{j=1}^6 |l_{j,i_j}(\vec{x}^j(\vec{\beta}^{*j}))|^2. \quad (129)$$

We now study the term by term the quantities in this expression.

$$\begin{aligned} |B(\vec{\beta}^*)| &= \prod_{j=1}^6 |B_j(\vec{\beta}^{*j})| \\ &= \prod_{j=1}^6 |e^{\frac{1}{2}n_j \vec{\beta}^{*j}}| \\ &= \left| \left(\frac{1}{\sqrt{-i(1+\epsilon)}} \right)^{n_1/2} \left(\frac{1}{\sqrt{i(1-\epsilon)}} \right)^{n_2/2} \left(\frac{1}{\sqrt{i(1+\epsilon)}} \right)^{n_3/2} \left(\frac{1}{\sqrt{-i(1-\epsilon)}} \right)^{n_4/2} \right| \\ &= \frac{1}{(1-\epsilon^2)^{(L+L')|\Lambda|}}. \end{aligned} \quad (130)$$

Then:

$$\begin{aligned} |B(\vec{\beta}_{\vec{i}})^{-1}| &= \prod_{j=1}^6 |B_j(\vec{\beta}_{i_j}^j)^{-1}| \\ &= \prod_{j=1}^6 |e^{-\frac{1}{2}n_j \vec{\beta}_{i_j}^j}| \\ &= \prod_{j=1}^6 x_{j,i_j}^{n_j/2} \\ &= \prod_{j=1}^6 \left(\frac{i_j}{n_j+1} \right)^{n_j/2}. \end{aligned} \quad (131)$$

We now turn to each term $|l_{j,i_j}(\vec{x}^j(\vec{\beta}^{*j}))|$ for each fixed j :

$$\begin{aligned} l_{j,i_j}(\vec{x}^j(\vec{\beta}^{*j})) &= \prod_{\substack{k_j=1 \\ k_j \neq i_j}}^{n_j+1} \frac{|\vec{x}^j(\vec{\beta}^{*j}) - x_{j,k_j}|}{|x_{j,i_j} - x_{j,k_j}|} \\ &= (n_j+1)^{n_j} \frac{\frac{1}{\sqrt{(\rho_j \cos \theta_j - \frac{i_j}{n_j+1})^2 + \rho_j^2 \sin^2 \theta_j}} \prod_{k_j=1}^{n_j+1} \sqrt{(\rho_j \cos \theta_j - \frac{k_j}{n_j+1})^2 + \rho_j^2 \sin^2 \theta_j}}{\prod_{k_j=1}^{i_j-1} (i_j - k_j) \prod_{k_j=i_j+1}^{n_j+1} (k_j - i_j)} \\ &\leq (n_j+1)^{n_j} \frac{\frac{1}{\sqrt{(\rho_j \cos \theta_j - \frac{i_j}{n_j+1})^2 + \rho_j^2 \sin^2 \theta_j}} e^{\frac{n_j+1}{2} I(\rho_j, \theta_j)}}{i_j! (n_j+1-i_j)!}, \end{aligned} \quad (132)$$

where $\vec{x}^j(\vec{\beta}^{*j}) \equiv \rho_j e^{i\theta_j}$ as can be deduced by looking at Eqs. 55, 59 and:

$$I(\rho_j, \theta_j) = \int_0^1 dx \log [(\rho_j \cos \theta_j - (x - \frac{1}{n_j+1}))^2 + \rho_j^2 \sin^2 \theta_j] < -\frac{1}{4}. \quad (133)$$

The last inequality holds for the cases considered by Eq. 59, for $n_j \geq 10$. Note that $\theta_1 = -\theta_2 = -\theta_3 = \theta_4 = \frac{\pi}{4}$ and $\theta_5, \theta_6 \ll 1$ since $J\tau/L, J\tau'/L' \ll 1$ by assumption in the adiabatic mapping. By reassembling everything together and from Eq. 129 we get:

$$\sigma_f^2 \leq \sum_{\vec{i}} A_{\vec{i}}^2 \delta_{\vec{i}}^2, \quad (134)$$

with:

$$\begin{aligned} A_{\vec{i}}^2 &= \frac{\prod_{j=1}^6 \left[\frac{\left(\frac{i_j}{n_j+1} \right)^{n_j} (n_j+1)^{2n_j} e^{(n_j+1)I(\rho_j, \theta_j)}}{\left((\rho_j \cos \theta_j - \frac{i_j}{n_j+1})^2 + \rho_j^2 \sin^2 \theta_j \right) (i_j! (n_j+1-i_j)!)^2} \right]}{(1-\epsilon^2)^{2(L+L')|\Lambda|} 2^{2(L+L'+1)|\Lambda|}} \\ &\leq \frac{1}{(1-\epsilon^2)\theta_5^2\theta_6^2 \sin^8 \frac{\pi}{4}} \frac{\prod_{j=1}^6 \left[\frac{\left(\frac{i_j}{n_j+1} \right)^{n_j} (n_j+1)^{2n_j} e^{-(n_j+1)/4}}{(i_j! (n_j+1-i_j)!)^2} \right]}{(1-\epsilon^2)^{2(L+L')|\Lambda|} 2^{2(L+L'+1)|\Lambda|}}. \end{aligned} \quad (135)$$

In arriving at the inequality above we used the fact that $(\rho_j \cos \theta_j - \frac{i_j}{n_j+1})^2 + \rho_j^2 \sin^2 \theta_j \geq \rho_j^2 \sin^2 \frac{\pi}{4}$ for $j = 1, 2, 3, 4$ and $(\rho_j \cos \theta_j - \frac{i_j}{n_j+1})^2 + \rho_j^2 \sin^2 \theta_j \geq \theta_j^2$ for $j = 5, 6$, supposing that $\theta_5, \theta_6 \rightarrow 0$ as is the case. In the “temperature domain” this formula reads:

$$A^2(\beta_{i,j}) = \frac{1}{\theta_5^2 \theta_6^2 \sin^8 \frac{\pi}{4}} \frac{\prod_{j=1}^6 \left[\frac{e^{-n_j \beta_{j,i_j}} (n_j+1)^{2n_j} e^{-(n_j+1)/4}}{\Gamma^2((n_j+1)e^{-\beta_{j,i_j}}+1) \Gamma^2((n_j+1)-(n_j+1)e^{-\beta_{j,i_j}}+1)} \right]}{(1-\epsilon^2)^{2(L+L'+1)} |\Lambda| 2^{2(L+L'+1)} |\Lambda|} . \quad (136)$$

From this we can get the following condition for the variance on the overlap to be polynomially bounded in the system size expressed for generic temperatures:

$$\delta(\vec{\beta}) \leq \frac{1}{A(\vec{\beta})} . \quad (137)$$

Explicitly we have:

$$\delta(\vec{\beta}) \leq \theta_5 \theta_6 \sin^4 \frac{\pi}{4} \prod_{j=1}^6 \frac{e^{\frac{n_j+1}{8}} \Gamma((n_j+1)e^{-\beta_j}+1) \Gamma((n_j+1)-(n_j+1)e^{-\beta_j}+1)}{(n_j+1)^{n_j} e^{-\frac{n_j}{2} \beta_j}} , \quad (138)$$

where we used $1 - \epsilon^2 \geq \frac{1}{2}$. By using Stirling approximation we then get:

$$\log \delta(\vec{\beta}) \leq \sum_{j=1}^6 n_j \left(g(\beta_j) + \frac{\beta_j}{2} \right) + \sum_{j=1}^6 \log(n_j+1) + \sum_{j=1}^6 g(\beta_j) + K , \quad (139)$$

where:

$$\begin{aligned} g(\beta_j) &= (1 - e^{-\beta_j}) \log(1 - e^{-\beta_j}) - \beta_j e^{-\beta_j} - \frac{7}{8} \\ K &= 4 \log \sin \frac{\pi}{4} + \log \theta_5 \theta_6 . \end{aligned} \quad (140)$$

This result is telling us how much error we can tolerate in the sampling of the classical partition function in order to be able to reconstruct certain quantum overlaps with a precision that scales polynomially in the system size. All error values satisfying Eq. 139 allow for such a reconstruction. For this reason, if we want to obtain a weaker but more compact result we can chose to state a smaller threshold. We can do this by substituting the functions appearing in Eq. 139 with their minimum (see Fig. G) getting to:

$$\log \delta(\vec{\beta}) \leq \sum_{j=1}^6 \left(\frac{\beta_j}{2} + a \right) n_j + \sum_{j=1}^6 \log(n_j+1) + b , \quad (141)$$

where:

$$a \leq \min_{\beta} g(\beta) \sim -1.6 \quad (142)$$

$$b = K - 10 . \quad (143)$$

In the thermodynamic limit the above formula can be further approximated by:

$$\begin{aligned} \log \delta(\vec{\beta}) &\leq \sum_{j=1}^6 \left(\frac{\beta_j}{2} + a \right) n_j + \sum_{j=1}^6 \log(n_j+1) + \log \theta_5 \theta_6 \\ &< \sum_{j=1}^6 \left(\frac{\beta_j}{2} + a \right) n_j + \sum_{j=1}^6 \log(n_j) + \log \theta_5 \theta_6 , \end{aligned} \quad (144)$$

so that:

$$\delta(\vec{\beta}) \leq 2^4 (JT)(J'T') L(L-1) L'(L'-1) |\Lambda|^6 \prod_{j=1}^6 e^{\left(\frac{\beta_j}{2} - 1.6\right) n_j} . \quad (145)$$

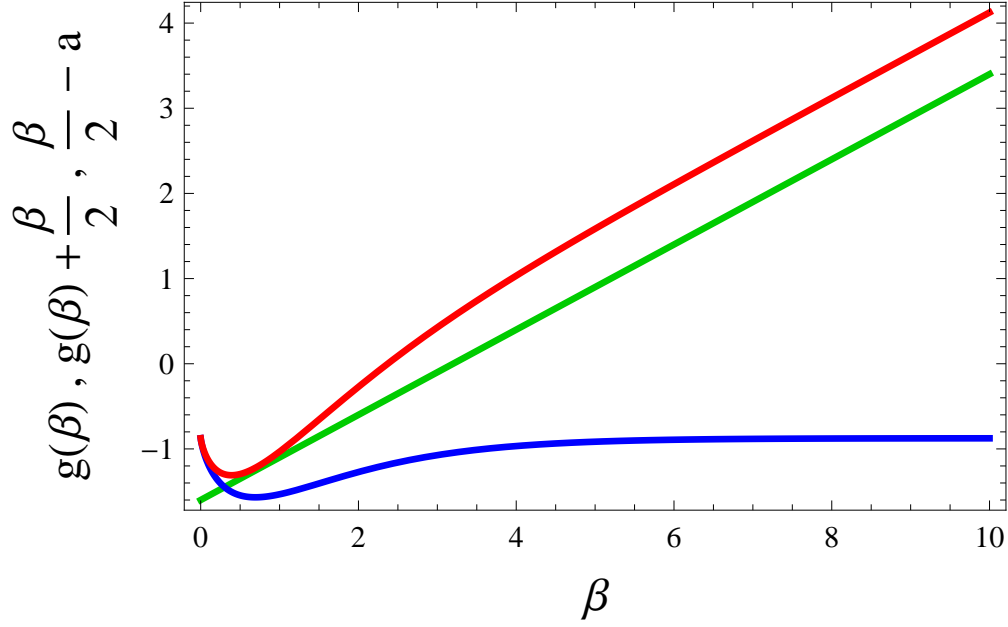


Figure 9: Function $g(\beta)$ (blue) and $g(\beta) + \frac{\beta}{2}$ (red) and $\frac{\beta}{2} - a$ with $a = \min_{\beta} g(\beta) = -1.6$ as a function of β .

References

- [1] D. Aharonov, V. F. R. Jones, and Z. Landau, Symposium on the Theory of Computing, Hobart, Australia (2006), quant-ph/0511096.
- [2] G. De las Cuevas, W. Dür, M. Van den Nest, and M.A. Martin-Delgado, New J. Phys. **13**, 093021 (2011).
- [3] I. Arad and Z. Landau, SIAM J. Comput. **39**, 3089 (2010)
- [4] D. Aharonov, I. Arad, E. Eban and Z. Landau, quant-ph/0702008 (2007).
- [5] W. Lenz, Physikalische Zeitschrift **21**, 613-615 (1920).
- [6] P. DiFrancesco, P. Matthieu, and D. Sénéchal, *Conformal Field Theory*, Springer (1996).
- [7] F. Barahona, J. Phys. A **15** 3241-3253 (1982).
- [8] G. De las Cuevas, W. Dür, M. Van den Nest, and M.A. Martin-Delgado, New J. Phys **13**, 093021 (2011).
- [9] M. Bremner, R. Jozsa, and D.J. Sheperd, Proc. R. Soc. A **467**, 459 (2011).
- [10] A. Razborov, Q. Inf. Comp. **4** 222 (2004).
- [11] J. Preskill, arXiv:1203.5813.
- [12] G. K. Brennen, Q. Inf. Comp. **3**, 619 (2003).
- [13] S.C. Benjamin, Phys. Rev. A **61**, 020301R (2000).

- [14] R. Raussendorf, Phys. Rev. A **72**, 052301 (2005).
- [15] J. Fitzsimons and J. Twamley, Phys. Rev. Lett. **97**, 090502 (2006).
- [16] L. Jiang, G. K. Brennen, A. V. Gorshkov, K. Hammerer, M. Hafezi, E. Demler, M. D. Lukin, and P. Zoller, Nature Phys. **4**, 482 (2008).
- [17] G.K. Brennen, K. Hammerer, L. Jiang, M.D. Lukin, and P. Zoller, arXiv:0901.3920.
- [18] R.K. Bathia, *Statistical Mechanics*, 2nd ed., Butterworth-Heinemann, Oxford (1996).
- [19] C.P. Master, F. Yamaguchi, and Y. Yamamoto, Phys. Rev. A **67**, 032311 (2003).
- [20] M.-H. Yung, D. Nagaj, J.D. Whitfield, and A. Aspuru-Guzik, Phys. Rev. A **82**, 060302(R) (2010).
- [21] W. Dür and M. Van den Nest, Phys. Rev. Lett. **107**, 170402 (2011).
- [22] W. Feller, *An Introduction to Probability Theory and Its Applications*, Volume II, 2nd ed., John Wiley & Sons, New York (1972).
- [23] F. Y. Wu and C.N. Yang, *Exactly solved models: a journey in statistical mechanics*, World Scientific, Singapore (2009).
- [24] F. Jaeger, D.L. Vertigan, and D.J.A. Welsh, Math. Proc. of Camb. Phil. Soc. **108**, 35 (1990).
- [25] G Paz-Silva, G.K. Brennen, and J. Twamley, Phys. Rev. A **80**, 052318 (2009).
- [26] M. Jerrum and A. Sinclair, SIAM J. on Compt. **22**, 1087 (1993).
- [27] L.A. Goldberg and M. Jerrum, J. Combinatorics, Probability, and Computing **16**, 43 (2007).
- [28] P. Zanardi and N. Paunkovic, Phys. Rev. E **74**, 031123 (2006).
- [29] A. Ambainis and O. Regev, quant-ph/041152.
- [30] S-J. Gu, Int. J. Mod. Phys. B **24**, 4371 (2010).
- [31] J. B. Kogut, Rev. Mod. Phys. **51**, 659 (1979).
- [32] E. Fradkin and L. Susskind, Phys. Rev. D **17**, 2637 (1978).
- [33] K.C. Chung and T.H. Yao, SIAM J. on Num. Anal. **14**, 735 (1977).
- [34] W. Dür and M. Van den Nest, Phys. Rev. Lett. **107**, 170402 (2011).
- [35] P. Wocjan, C-F. Chiang, A. Abeyesinghe, and D. Nagaj, Phys. Rev. A **80**, 022340 (2009).
- [36] J. Simon, W.S. Bakr, R. Ma, M. E. Tai, P.M. Preiss, and M. Greiner, Nature **472** 307 (2011).
- [37] I. Buluta, S. Ashhab, and F. Nori, Rep. Prog. Phys. **74**, 104401 (2011).
- [38] G.A. Paz-Silva, G.K. Brennen, and J. Twamley, New J. Phys. **13**, 013011 (2011).
- [39] P. Hauke, F.M. Cucchietti, L. Tagliacozzo, I.H. Deutsch, and M. Lewenstein, Rep. Prog. Phys. **75**, 082401 (2012).
- [40] K.R. Brown, R.J. Clark, and I.L. Chuang, Phys. Rev. Lett. **97**, 050504 (2006).

- [41] Andreas Galanis, Daniel Stefankovic, Eric Vigoda, arXiv:1203.2226.
- [42] I.G. Shevtsova, Doklady Mathematics **82** (3), 862864 (2010).
- [43] P. Oscar Boykin, T. Mor, M. Pulver, V. Roychowdhury, and F. Vatan, In Proc. 40th FOCS, 486 (1999).
- [44] M.A. Nielsen and I. L. Chuang, *Quantum Computation and Quantum Information*, Cambridge University Press (2000).
- [45] W. van Dam, M. Mosca, and U. Vazirani, Proceedings of the 42nd Annual Symposium on Foundations of Computer Science, pp. 279-287 (2001), arXiv quant-ph/0206003.